# CONSTRUCTING VOLATILITY SURFACES FOR MANAGED FUNDS

**Trevor Joseph Brinkmann**



A dissertation submitted to the Department of Actuarial Science, Faculty of Commerce, at the University of Cape Town, in partial fulfilment of the requirements for the degree of Master of Philosophy.

22nd May 2014

*Master of Philosophy specializing in Mathematical Finance,*
*University of Cape Town,*
*Cape Town, South Africa*

# Declaration

I declare that this dissertation is my own, unaided work. It is being submitted for the Degree of Master of Philosophy at the University of Cape Town. It has not been submitted before for any degree or examination in any other university.

_____

22nd May 2014

# Abstract

In this dissertation, a methodology is developed for constructing a volatility surface for a managed fund by extending the work of Bakshi *et al.* (2003) and Taylor (2014). The power utility assumption (with constant relative risk aversion for a specific maturity) and historical returns series data are used for the identified factors influencing the return of the fund and the fund itself. The coefficient of relative risk aversion for a specific maturity and market is estimated from quoted option prices on a market index. This is used in combination with the identified factors and fund return series to estimate the risk-neutral skewness of the fund. An optimisation procedure is then used to determine the volatility smile of the fund for a specific maturity. Thereafter, the volatility surface of the fund is constructed by repeating each step for different maturities. Although this methodology produces sensible results, the optimisation routine used is sensitive to initial values and constraints.

# Acknowledgements

Foremost, I would like to express my sincere gratitude to my advisors Dr. Marchand van Rooyen and Paolo Innocenzi for their guidance and patience. In addition, I would like to thank Professor David Taylor for his advice as well as for putting together the structure and resources that allowed this dissertation to be accomplished. I would also like to thank my family and fellow classmates for their support.

# Contents

# List of Figures

# List of Tables

# Chapter 1

# Introduction

The option pricing framework of Black and Scholes (1973) and Merton (1973) assumes that the underlying asset price follows geometric Brownian motion (and the log-return is normally distributed under the risk-neutral measure). This has become the canonical model for option pricing. Consequently, most markets quote call and put option prices in terms of a single number - the implied volatility. This is the input into the Black-Scholes-Merton (BSM) formula that corresponds to an option's price, which shall be denoted as the BSM implied volatility. It can be used as a substitute to price since there is a strictly increasing and convex relationship between the price of an option and the BSM implied volatility, meaning there is a one-to-one mapping between them.

In the BSM option pricing framework, the volatility parameter is assumed to be constant, resulting in a flat (i.e. constant) implied volatility surface - the implied volatility as a function of term and strike price. However, after the equity market crash of 1987 it was observed that BSM implied volatilities (often seen as just Black-Scholes volatilities in the literature) vary according to term and strike price (see, for example, Rubinstein (1994), Jarrow *et al.* (2007) and Tompkins (2001)). Recently, it was noted in Kotzé *et al.* (2013) that this phenomenon now exists in equity options, interest rate options, currency options and almost every other volatility market in the world. It has been shown that the log-normal assumption underpinning the Black-Scholes-Merton framework is often inaccurate (see, for example, Homescu (2011), Macbeth and Merville (1979) and Rubinstein (1985)). Furthermore, it was noted in Kotzé *et al.* (2013) that the structure of the volatility surface is directly

related to the non-normality of the risk-neutral distribution of the underlying asset. Consequently, we expect that a managed fund, consisting of a variety of assets, would possess a volatility surface dependent on term and strike price.

Many insurance companies offer financial products related to a managed fund, which contain embedded guarantees based on the investment performance of this fund. Such guarantees take many forms, with a common example being a guarantee on the capital invested (see Hardy (2003), for a list of several such guarantees). These investment guarantees are essentially financial derivatives where the underlying asset is the managed fund. In general, there is a small probability that the investment guarantee will have a non-zero payoff. This is because there is a small probability of the investment performance of the fund being poor enough to invoke the guarantee. In the terminology of option pricing, the guarantees are usually deep out-of-the-money. This has resulted in complacency in the past. However, it is noted in Hardy (2003) that the risk management of these guarantees now represents a major test of insurance companies.

One reason for investment-linked insurance guarantees becoming more prominent may be the movement of pensions from defined benefit schemes to defined contribution schemes. Under defined benefit schemes a pensioner receives a known final benefit (usually a function of salary before retirement) and the contributions are uncertain. Historically, the risk of these benefit schemes were borne by the employer since they would cover any shortfalls between the benefits (i.e. the liabilities) and the assets backing these. In contrast, under a defined contribution scheme, the final benefit is unknown (since it is dependent on future investment performance) and the contributions are usually related to salary (see Deelstra *et al.* (2004) for further detail). In this instance, the risk of the resulting investment performance, and consequently the benefit at retirement, is borne by the employee. In order to address this uncertainty, insurance companies increased the number of guarantees offered to policyholders. In doing so, these insurance companies shift some of the risks from the policyholder to themselves. By supplying this investment guarantee, the insurance company is creating and providing an economic good to policyholders who, as individuals, would be unable to create such a product for themselves. In ad-

dition, insurance companies also attract more business by offering these guarantees, which contributes to increased profits.

A second reason investment-linked insurance guarantees have become more prominent may be the considerable development of financial derivatives being coupled with the principle of hedging. This advancement provided the necessary tools for effective risk management (i.e. costing and hedging) when writing such guarantees.

Insurance companies have traditionally reserved capital to act as a buffer against possible adverse market movements which may result in investment guarantees becoming material. The amount of capital is often stipulated by regulators through some form of prescribed formula irrespective of the risk of the particular product or its design. This is done as the regulators want to ensure insurance companies remain solvent and are able to deliver on their promises to policyholders during periods of market stress. It has now become common for these companies to use a dynamic-hedging approach, which was developed in financial derivative markets, in order to reduce the cost and risk of providing investment guarantees (Greenbaum and Ravindran (2002), Mueller *et al.* (2002) and Hardy (2003)). This is where a changing number of assets are held over time in order to replicate the guarantee payoff. This approach allows the insurance company to lower the statutory reserves (as stipulated by regulators) for providing investment guarantees, thus freeing up capital to be used elsewhere. Furthermore, this approach reduces the cost of providing these investment guarantees, which should directly benefit both the policyholders and shareholders of the insurance company.

Throughout this dissertation reference is made to the terms "volatility surface" and "volatility smile" and these relate specifically to the implied volatility surface or implied volatility smile. This must not be confused with the local volatility surface or local volatility smile. For details of the differences between implied and local volatility see Derman *et al.* (1996).

This dissertation details one possible method for constructing an implied volatility surface for a managed fund in the absence of an options market on this fund. This volatility surface will aid the pricing and hedging of investment guarantees on such a fund. In particular, this will allow a price to be placed on guarantees, which

better reflects the risk of the product, as well as aid in determining suitable hedging portfolios. This can be done by calibrating stochastic models, which are more complex than geometric Brownian motion, but more realistic, (such as a jump-diffusion model presented in Merton (1976), the model of Heston (1993) or the SABR model presented in Hagan *et al.* (2003)) to the volatility surface. A suitable method, such as Monte Carlo simulation, can then be used to price the guarantee and calculate the sensitivities of this price to changes in parameters of the model (i.e. the "Greeks"), which are then used when determining a hedge portfolio.

There are a number of complexities encountered when trying to construct a volatility surface for a managed fund. For example, there are no liquid markets for options written on managed funds. Therefore, there are no observable transactions and hence no observable implied volatilities for a managed fund. This means there are no observable points from which to begin to build a volatility surface. Moreover, since there is no active market in options related to a managed fund, there is no mechanism of arbitrage that would correct mispricings.

An additional challenge is that managed funds are comprised of different assets. Specifically, these funds may be made up of equities (listed or unlisted), index funds, derivatives, project finance assets, income-bearing assets and long dated asset-backed debt instruments, as well as many more possibilities. Implied volatilities of each constituent cannot be added together to determine the implied volatility of the fund due to the non-linear relationship between the volatility of a fund and the volatilities of its constituents. In addition, there may not even be option markets for the constituent assets, and thus no observable implied volatilities for these assets with which to work with. Moreover, some of the assets may be non-listed and/or are only marked-to-market infrequently making it difficult to place a value on them on a regular basis.

In addition, the composition of a managed fund may change at the discretion of the fund manager, meaning that the relative weighting of the assets within the fund can change on a regular basis without it being public knowledge.

Notably, the investment guarantees provided by insurance companies often are very long-term in nature. As a result, there is a large interest rate exposure in

these products, which contributes a great deal to the variability of the price of such a guarantee. This makes hedging out interest rate exposure a crucial facet of risk management on a long-dated insurance guarantee.

It should be noted that insurance companies may be able to dynamically, Delta-hedge the guarantees that they write on managed funds by transacting in the underlying managed fund itself. However, there may be statutory restrictions prohibiting the insurance company from transacting in the managed fund beyond a certain point. In this case, insurance companies may be required to use proxies for the underlying fund's constituents, and then transact in these assets, when necessary, in order to cross-hedge. Managed funds each have their own mandate that specifies the benchmark portfolio it is assessed against. The extent to which a managed fund follows the benchmark portfolio depends on the mandate of the fund and the allowance given to it to deviate from its benchmark. Consequently, this may assist in specifying a proxy-hedging strategy. This dissertation will discuss how having proxies which accurately describe a managed fund may assist in constructing the fund's volatility surface.

The focus of this dissertation is to present an economically and mathematically sound approach to constructing a volatility surface for a managed fund by making use of the theory developed by Bakshi *et al.* (2003) and the ideas subsequently used by Taylor (2014). Other methodologies in the world of implied volatility surface generation can be found in de Araújo and Maré (2006) and Flint *et al.* (2012), which focus on historical risk-neutral return distributions.

There are three results in Bakshi *et al.* (2003) which form the fundamental building blocks of the methodology presented in this dissertation. The first is the relationship linking, in a model-independent manner, the risk-neutral skewness of a security (i.e. the normalised third central moment of the risk-neutral distribution of the underlying security) to a continuum of option prices on this security. The second result requires the assumption that the power utility function represents the preferences of a particular market. In this case, a relationship was established between the risk-neutral skewness of a security and the real-world (physical) moments of the security. The last result is unearthed if the return of a security is assumed to

be linearly related to a number of factors. Under this assumption, the risk-neutral skewness of the security is found to be related to the risk-neutral skewness of each factor. This is used in this dissertation, where it is assumed that a combination of factors have been identified, which together accurately explain the return of the fund. These factors will be referred to as the influential factors (i.e. factors that influence the return of the fund).

In order to avoid confusion, the term skew or skewness will only be used when referring to the third moment of a random variable. Furthermore, the cross section of the volatility surface at a particular maturity, will be referred to as the volatility smile, or simply the smile. In the literature however, what is here termed the smile may be referred to as the volatility skew.

The methodology presented in this paper details how to find the volatility smile, for a particular maturity, for a managed fund. This can then be repeated for different maturities to produce a volatility surface. In particular, for a specific maturity, it is assumed that the power utility function represents the preferences of a particular market. This parameter is estimated using historical returns series for a market index along with quoted option prices on this market index. The risk-neutral skewness for each influential factor is then calculated. This is done using one of two methods. If the influential factor has an observable options market, its risk-neutral skewness is calculated from quoted options prices. If there is no such market for this influential factor then the historical returns series for this factor in combination with the estimated utility function are used to determine its risk-neutral skewness. Following this, the risk-neutral skewness for each influential asset is combined in a non-linear manner to calculate the risk-neutral skewness for the fund. Finally, an optimisation procedure is used to determine the optimal volatility smile that conforms to the risk-neutral skewness of the fund, using a quadratic (or other) functional form for the volatility smile.

The practical example presented in this dissertation made use of a quadratic volatility smile in moneyness for all assets. However, other functional forms could have been used, such as an exponential or spline, to represent the volatility smile. Moreover, one functional form does not need to be assumed for all assets/factors, and

a different functional form could be used for each asset/factor involved, if wanted. The methodology detailed in this dissertation is for a generic volatility smile.

The rest of this dissertation is structured as follows: Chapter 2 reviews the theory that forms the basis of this dissertation. Chapter 3 details a methodology that can be used to construct a volatility surface for a managed fund and possible obstacles that may be encountered when trying to implement this methodology. Chapter 4 applies the methodology of Chapter 3 in a practical scenario. Finally, the conclusions of this dissertation are presented in Chapter 5.

# Chapter 2

# Review of Theory

## 2.1 Notation

Throughout this dissertation the following notation is adopted. The price of security $i$ at time $t$ is given by $S_t^{(i)}$ and its continuously-compounded dividend yield is $q^{(i)}$ for $i = 1, ..., N$. Furthermore, it is assumed that all securities are positive with a probability of 1 for all time horizons. Without loss of generality, the risk-free continuously-compounded rate of interest will be denoted $r$, a constant.

For the rest of this section the necessary theory will be presented for a specific security (i.e. for a particular $i$) and therefore the superscript $i$ will be dropped. Let the risk-neutral density of the price of a security over the period $t$ to $T$ be given by $\mathbb{Q}(t, T, S)$, which may often be written as just $q(S_T)$. In addition, the real-world (i.e. physical) density for a particular security is similarly given by $\mathbb{P}(t, T, S)$, or simply $p(S_T)$. For more on the risk-neutral and real-world (physical) measures and their uses in pricing and hedging of financial derivatives see Bjork (2009), Bingham and Rudiger (2004), Shreve (2004a) and Shreve (2004b).

This dissertation will only deal with payoffs occurring at time $T$, that are integrable with respect to the risk-neutral density (i.e. $\int_0^\infty |H(S_T)|\, \mathbb{Q}(S_T)\, dS_T < \infty$ for payoff $H(S_T)$ ). The risk-neutral expectation, as at time $t$, of this payoff will be represented by $\mathbb{E}_t^{\mathbb{Q}}[\cdot]$ (i.e. $\mathbb{E}_t^{\mathbb{Q}}[H(S_T)] = \mathbb{E}^{\mathbb{Q}}[H(S_T)|\mathcal{F}_t] = \int_0^\infty H(S_T)\mathbb{Q}(S_T)dS$, where $\mathcal{F}_t$ is the filtration of asset $i$ up to time $t$).

With this notation, European call and put option prices, as at time $t$ with ma-

turity $T$ and strike price $K$, can be written as:

$$\begin{aligned} C(t,T;K) &= \int_0^\infty e^{-r(T-t)} \max(S_T - K, 0)\ \mathbb{Q}(S_T)\, dS_T \\ &= \mathbb{E}_t^{\mathbb{Q}}[e^{-r(T-t)} \max(S_T - K, 0)] \\ P(t,T;K) &= \int_0^\infty e^{-r(T-t)} \max(K - S_T, 0)\ \mathbb{Q}(S_T)\, dS_T \\ &= \mathbb{E}_t^{\mathbb{Q}}[e^{-r(T-t)} \max(K - S_T, 0)] \end{aligned}$$

respectively.

If there is a BSM implied volatility, $\sigma_{BSM}(t,T,K)$, at a specific time $t$ with maturity $T$ and strike price $K$, then the call and put option prices on a particular security are then:

$$C(t,T;K) = S_t e^{-q(T-t)}\Phi(d_1) - Ke^{-r(T-t)}\Phi(d_2) \tag{2.1}$$

$$P(t,T;K) = Ke^{-r(T-t)}\Phi(-d_2) - S_t e^{-q(T-t)}\Phi(-d_1) \tag{2.2}$$

where

$$\begin{aligned} d_1 &= \frac{\ln(\frac{S}{K}) + \left(r - q + \sigma_{BS}^2(t,T,K)/2\right)(T-t)}{\sigma_{BS}(t,T,K)\sqrt{(T-t)}} \\ d_2 &= \frac{\ln(\frac{S}{K}) + \left(r - q - \sigma_{BS}^2(t,T,K)/2\right)(T-t)}{\sigma_{BS}(t,T,K)\sqrt{(T-t)}} = d_1 - \sigma_{BS}(t,T,K)\sqrt{(T-t)} \end{aligned}$$

and $\Phi(\cdot)$ represents the cumulative standard Normal distribution function. A derivation of this can be found in Shreve (2004b) on page 238.

Later on, reference will be made to "moneyness", which will be represented by $m$. This is defined as the strike price of an option divided by the current price of the asset underlying the option, i.e. $m = \frac{K}{S_t}$. Implied volatility smiles are then defined to be functions relating the implied volatility of a security to moneyness (for a particular maturity), where the independent variable is moneyness. This implied volatility smile in moneyness format is also known as the relative or floating skew. Furthermore, the implied volatility smile for asset $i$ will be represented by $\sigma_i(m)$.

## 2.2 Recovering a Payoff (Bakshi and Madan (2000))

In this section the necessary theory presented in Bakshi and Madan (2000) is summarised. This theory is a building block of both Bakshi *et al.* (2003) and this dissertation.

Through the use of characteristic functions and Fourier analysis, the collection of twice-continuously differentiable payoff functions can be recovered through a continuum of out-the-money European put and call options. Specifically, Theorem 1 established that any payoff function belonging to the set of twice-continuously differentiable functions, $H(S_T) \in C^2$, adheres to the following:

$$\begin{aligned} H(S_T) =& H(\bar{S}) + (S_T - \bar{S})\frac{dH}{dS_T}(S_T)\Big|_{\bar{S}} + \int_{\bar{S}}^{\infty} \frac{d^2H}{dS_T^2}(S_T)\Big|_K \max(S_T - K, 0)\, dK \\ &+ \int_0^{\bar{S}} \frac{d^2H}{dS_T^2}(S_T)\Big|_K \max(K - S_T, 0)\, dK \end{aligned}$$

for some $\bar{S}$ and strike price $K$. It is noted that the maximum terms in the above formula are European call and put option payoffs. This equation is described intuitively as being able to buy the curvature of the payoff function with call and put options.

A discount factor is now applied to both sides of this equation along with the risk-neutral expectation operator, $\mathbb{E}_t^{\mathbb{Q}}[\cdot]$, to get:

$$\begin{aligned} \mathbb{E}_t^Q[e^{-r(T-t)}H(S_T)] = &\left(H(\bar{S}) - \bar{S}\frac{dH}{dS_T}(S_T)\Big|_{\bar{S}}\right) e^{-r(T-t)} + S_t\frac{dH}{dS_T}(S_T)\Big|_{\bar{S}} \\ &+ \int_{\bar{S}}^{\infty} \frac{d^2H}{dS_T^2}(S_T)\Big|_K C(t,T,K)dK \\ &+ \int_0^{\bar{S}} \frac{d^2H}{dS_T^2}(S_T)\Big|_K P(t,T,K)dK \end{aligned} \tag{2.3}$$

This results because $\mathbb{Q}$ is the risk-neutral (i.e. equivalent martingale) measure and so $\mathbb{E}_t^Q[e^{-r(T-t)}S_T] = S_t$.

This is a powerful result. It allows the theoretical synthesising of any twice differentiable payoff, on a particular underlying security, in a model independent manner. Specifically, this can be done with a combination of appropriate holdings

in a zero-coupon bond, the security underlying the payoff, and a linear combination of call and put options written on the underlying security. The remarkable feature of this result is that it is independent of the model chosen to represent the underlying asset price process.

## 2.3 Theory presented in Bakshi *et al.* (2003)

The relevant theory found in Bakshi *et al.* (2003) is presented in the sub-headings headings below.

### 2.3.1 Recovering Risk-Neutral Moments

In this section, equation (2.3) is exploited in order to synthesise risk-neutral moments, for a particular term, of an underlying asset from its traded option prices. In particular, the formulae for the risk-neutral variance, skewness and kurtosis are found using the theory of the previous section.

Formally, for a particular security $i$, the log capital-return over the period $t$ to $T$, with price $S_t$ at time $t$, is defined by $R(t,T) \equiv \ln(\frac{S_T}{S_t})$. The following payoff functions/contracts and their discounted values are then defined as follows:

- variance contract: $H(S_T) = (R(t,T))^2$, with price

$$V(t,T) \equiv \mathbb{E}_t^{\mathbb{Q}}[e^{-r(T-t)}(R(t,T))^2] \tag{2.4}$$

- cubic contract: $H(S_T) = (R(t,T))^3$, with price

$$W(t,T) \equiv \mathbb{E}_t^{\mathbb{Q}}[e^{-r(T-t)}(R(t,T))^3] \tag{2.5}$$

- quartic contract $H(S_T) = (R(t,T))^4$, with price

$$X(t,T) \equiv \mathbb{E}_t^{\mathbb{Q}}[e^{-r(T-t)}(R(t,T))^4] \tag{2.6}$$

It is noted that the definitions of $V(t,T), W(t,T)$ and $X(t,T)$ all contain a discount

term so that equation (2.3) can be used.

It is known that $\mathbb{E}_t^{\mathbb{Q}}[e^{-(r-q)(T-t)}S_T] = S_t$ and so:

$$\begin{aligned} e^{(r-q)(T-t)} &= \mathbb{E}_t^{\mathbb{Q}}\left[\frac{S_T}{S_t}\right] \\ &= \mathbb{E}_t^{\mathbb{Q}}[e^{R(t,T)}] \\ &\approx 1 + \mathbb{E}_t^{\mathbb{Q}}[R(t,T)] + \frac{1}{2}\mathbb{E}_t^{\mathbb{Q}}\left[(R(t,T))^2\right] + \frac{1}{6}\mathbb{E}_t^{\mathbb{Q}}\left[(R(t,T))^3\right] + \frac{1}{24}\mathbb{E}_t^{\mathbb{Q}}\left[(R(t,T))^4\right] \end{aligned} \tag{2.7}$$

where the last line follows from using a Taylor expansion of $e^x$ about 0 [1]. Recall that $r$ is assumed to be deterministic, which allows the above result to be attained. Rearranging equation (2.7) gives:

$$\mu(t,T) \equiv \mathbb{E}_t^{\mathbb{Q}}\left[\ln\left(\frac{S_T}{S_t}\right)\right] \tag{2.8}$$

$$\begin{aligned} &= \mathbb{E}_t^{\mathbb{Q}}[R(t,T)] \\ &\approx e^{(r-q)(T-t)} - 1 - \frac{e^{r(T-t)}V(t,T)}{2} - \frac{e^{r(T-t)}W(t,T)}{6} - \frac{e^{r(T-t)}X(t,T)}{24} \end{aligned} \tag{2.9}$$

where the continuous dividend yield, $q$, is included in this formulation. It is noted that $\mu(t,T)$ is the risk-neutral expectation of the log-capital-return and is thus called the (non-discounted) mean contract. It is further noted that it is not discounted as done for $V(t,T), W(t,T)$ and $X(t,T)$. Consequently, the coefficients of $V(t,T), W(t,T)$ and $X(t,T)$, in equation (2.9), all contain $e^{r(T-t)}$ in order to cancel the discounting term in their definitions. Thus, the first risk-neutral moment of the security is estimated in terms of its second, third and fourth risk-neutral moments. This estimate is found to be extremely accurate and including higher moments in the Taylor expansion estimate was found to add little to its accuracy.

Now set $\bar{S} = S_t$, so that $H(\bar{S}) = R(t,t) = \ln(\frac{S_t}{S_t}) = 0$, resulting in the first line of equation (2.3) to be:

$$\left(\left(0 - S_t\frac{dH}{dS_T}(S_T)\Big|_{\bar{S}}\right)e^{-(T-T)} + S_t\frac{dH}{dS_T}(S_T)\Big|_{\bar{S}}\right) = 0$$

[1] Taylor expansion of $e^x$ about 0 is given by $e^x = 1 + x + \frac{x^2}{2} + \frac{x^3}{6} + \frac{x^4}{24} + o(x^4)$, for small $x$.

This causes Equation (2.3) to become:

$$\begin{aligned}\mathbb{E}_t^Q[e^{-r(T-t)}H(S_T)] = &\int_{S_t}^{\infty} \frac{d^2H}{dS_T^2}(S_T)\Big|_K C(t,T,K)dK \\ &+ \int_0^{S_t} \frac{d^2H}{dS_T^2}(S_T)\Big|_K P(t,T,K)dK\end{aligned}$$

which can then be used to determine the prices of the variance contract ($V(t,T)$), the cubic contract ($W(t,T)$) and the quartic contract ($X(t,T)$). The second differentials of the various contracts are given by:

$$\frac{d^2H}{dS_T^2}(K) = \begin{cases} \dfrac{2\left(1-\ln\left(\frac{K}{S_t}\right)\right)}{K^2} & \text{variance contract} \\ \dfrac{6\ln\left(\frac{K}{S_t}\right) - 3\left(\ln\left(\frac{K}{S_t}\right)\right)^2}{K^2} & \text{cubic contract} \\ \dfrac{12\left(\ln\left(\frac{S_t}{K}\right)\right)^2 + 4\left(\ln\left(\frac{S_t}{K}\right)\right)^2}{K^2} & \text{quartic contract} \end{cases}$$

This results in the following contract prices:

$$\begin{aligned} V(t,T) = &\int_{S_t}^{\infty} \frac{2\left(1-\ln\left(\frac{K}{S_t}\right)\right)}{K^2} C(t,T,K)dK \\ &+ \int_0^{S_t} \frac{2\left(1-\ln\left(\frac{K}{S_t}\right)\right)}{K^2} P(t,T,K)dK \end{aligned} \tag{2.10}$$

$$\begin{aligned} W(t,T) = &\int_{S_t}^{\infty} \frac{6\ln\left(\frac{K}{S_t}\right) - 3\left(\ln\left(\frac{K}{S_t}\right)\right)^2}{K^2} C(t,T,K)dK \\ &+ \int_0^{S_t} \frac{6\ln\left(\frac{K}{S_t}\right) - 3\left(\ln\left(\frac{K}{S_t}\right)\right)^2}{K^2} P(t,T,K)dK \end{aligned} \tag{2.11}$$

$$\begin{aligned} X(t,T) = &\int_{S_t}^{\infty} \frac{12\left(\ln\left(\frac{S_t}{K}\right)\right)^2 + 4\left(\ln\left(\frac{S_t}{K}\right)\right)^2}{K^2} C(t,T,K)dK \\ &+ \int_0^{S_t} \frac{12\left(\ln\left(\frac{S_t}{K}\right)\right)^2 + 4\left(\ln\left(\frac{S_t}{K}\right)\right)^2}{K^2} P(t,T,K)dK \end{aligned} \tag{2.12}$$

With these contract prices, the $(T-t)$-period risk-neutral skewness, $SKEW(t,T)$,

is found to be given by:

$$\begin{aligned} SKEW(t,T) \equiv & \frac{\mathbb{E}_t^{\mathbb{Q}}\big[\,\big(\,R(t,T)-\mathbb{E}[R(t,T)]\,\big)^3\,\big]}{\Big\{\,\mathbb{E}_t^{\mathbb{Q}}\big[\,\big(\,R(t,T)-\mathbb{E}\big[R(t,T)\big]\,\big)^2\,\big]\,\Big\}^{\frac{3}{2}}} \\ = & \frac{e^{r(T-t)}\Big[W(t,T)-3\mu(t,T)V(t,T)\Big]+2\big(\,\mu(t,T)\,\big)^3}{\Big\{\,e^{r(T-t)}V(t,T)-\big(\,\mu(t,T)\,\big)^2\,\Big\}^{\frac{3}{2}}} \end{aligned} \tag{2.13}$$

and the risk-neutral kurtosis, $KURT(t,T)$, as

$$\begin{aligned} KURT(t,T) \equiv & \frac{\mathbb{E}_t^{\mathbb{Q}}\big[\,\big(\,R(t,T)-\mathbb{E}[R(t,T)]\,\big)^4\,\big]}{\Big\{\,\mathbb{E}_t^{\mathbb{Q}}\big[\,(R(t,T)-\mathbb{E}[R(t,T)])^2\,\big]\,\Big\}^2} \\ = & \frac{e^{r(T-t)}\,\Big[\,X(t,T)-4\mu(t,T)W(t,T)+6\big(\,\mu(t,T)\,\big)^2V(t,T)\Big]-3\big(\,\mu(t,T)\,\big)^4}{\Big\{\,e^{r(T-t)}V(t,T)-\big(\,\mu(t,T)\,\big)^2\,\Big\}^2} \end{aligned} \tag{2.14}$$

The second line for both $SKEW(t,T)$ and $KURT(t,T)$ follow from expanding the power in the numerator of the first lines and then substituting in the definitions of $V(t,T), W(t,T)$ and $X(t,T)$, as given in equations (2.4), (2.5) and (2.6). Similarly to above, the coefficients of $V(t,T), W(t,T)$ and $X(t,T)$ in equations (2.13) and (2.14) all contain the factor $e^{r(T-t)}$ in order to remove the discounting term in their definitions.

Consequently, given a continuum of option prices over the strike range $K \in (0,\infty)$, (or equivalently a continuum of BSM implied volatilities over the strike range) for a particular security and specific term, the risk-neutral moments of the security for this term can be found. This is a powerful tool that converts information in the market (i.e. BSM implied volatilities) into risk-neutral moments. What is also impressive is that this can be done without having to make any assumption about the return distribution of the underlying security. In other words, the characteristics of the risk-neutral return distribution can be determined in a model independent manner. This is extremely important, because if a specific distributional assumption

was made, this would influence both the risk-neutral moments themselves as well as the relationships between the various moments.

In a practical setting the above results can be used to approximate the risk-neutral skewness and kurtosis of a security. This was done for individual stock and index options traded on the Chicago Board Options Exchange risk-neutral skewness in Dennis and Mayhew (2002).

### 2.3.2 Sources of Risk-Neutral Skewness

This section considers how, under certain assumptions, the risk-neutral skewness of a security can be explained by the real-world moments of the security and risk aversion.

Specifically, let $p(R_i)$ be the real-world marginal probability density for the log-return of security $i$, $S^{(i)}$, for $i = 1, ..., N, M$ (where $M$ represents the market index), over the time period $t$ to $T$. In addition, let $p(R_1, ..., R_N, R_M)$ be the joint real-world probability density of all securities and the market index. In addition, let $q(\cdot)$ similarly represent both the marginal and joint probability densities under the risk-neutral measure.

Furthermore, assume a power utility function in wealth, i.e. a utility function, $U$, of the form

$$U(x) = \begin{cases} \dfrac{x^{1-\gamma} - 1}{1-\gamma} & \gamma > 0, \gamma \neq 1 \\ \ln(x) & \gamma = 1 \end{cases}$$

This class of utility functions displays constant relative risk aversion equal to $\gamma$, where the measure of relative risk aversion (also known as the Arrow-Pratt measure) is given by $\frac{-xU''(x)}{U'(x)}$ (see Appendix A for this derivation). For more about the characteristics of the power utility family of functions see Wakker (2008).

It is shown through the use of the Radon-Nikodym theorem that the risk-neutral

distribution is related to the real-world moments of the security as follows:

$$q(R_M) = \frac{e^{-\gamma R_M}\, p(R_M)}{\int e^{-\gamma R_M}\, p(R_M)\, dR_M} \tag{2.15}$$

$$q(R_1, ..., R_N, R_M) = \frac{e^{-\gamma R_M}\, p(R_1, ..., R_N, R_M)}{\int e^{-\gamma R_M}\, p(R_1, ..., R_N, R_M)\, dR_1, ...dR_n,\, dR_M} \tag{2.16}$$

where $\gamma$ is the coefficient of relative risk aversion and $e^{-\gamma R_M}$ is the pricing kernel in power utility economies. It is commented in Bakshi *et al.* (2003) on page 109 that the risk-neutral density is "obtained by exponentially tilting the physical density".

By assuming a power utility function and using the results of equations (2.15) and (2.16), Theorem 2 of the paper was established:

$$SKEW_M(t,T) \approx \overline{SKEW}_M(t,T) - \gamma(t,T)\left(\overline{KURT}_M(t,T) - 3\right)\overline{STD}_M(t,T) \tag{2.17}$$

where $\overline{STD}_M(t,T)$, $\overline{SKEW}_M(t,T)$ and $\overline{KURT}_M(t,T)$ are the market return standard deviation, skewness and kurtosis, under the real world probability measure, respectively. See Appendix B.1 for the derivation of this. In this dissertation, $\gamma$ is presented as being dependent on the time horizon (which was not done in Bakshi *et al.* (2003)) in order to accommodate differing levels of risk aversion for different time horizons.

Three contributing factors to negative risk-neutral skewness are pointed out, namely: a negative skewness in the real world distribution, a relatively high kurtosis of the real world distribution (i.e. fat-tailed distributions) and high standard deviation of the real-world distribution when the real world kurtosis is greater than 3 (i.e. when the distribution is fat-tailed).

This result of equation (2.17) can be used in combination with (2.13) to estimate the coefficient of relative risk aversion, $\gamma$, for a given time horizon as long as there are sufficient option prices (needed to calculate the risk-neutral skew - $SKEW$) and real-world distributional characteristics, namely the real-world standard deviation, skewness and kurtosis. It must be noted that equation (2.17) is only an approximation and thus $\gamma$ will also be an approximation.

It is shown that the above theorem can be generalised to a broader range of

marginal utility functions. These include hyperbolic absolute risk aversion (HARA) utility functions and bounded versions of the loss aversion utility functions of Kahneman and Tversky (1979). The power utility will henceforth be assumed for the rest of this dissertation.

### 2.3.3 Skew Laws

This section looks at what were termed the skew laws in Bakshi *et al.* (2003). In particular, it is assumed that the log-returns of a security are linearly related to a number of factors. It is then shown how the skewness of the security relates to the skewness of each of the factors, for both the real-world or risk-neutral measure. In Bakshi *et al.* (2003), this assumption was used to relate a constituent of a market index to the market index itself. In this dissertation, this assumption will be used later to relate the return of a managed fund to the return of factors that influence the return of the managed fund, (e.g. the benchmarks of the managed fund).

Specifically, begin by making the common assumption that the log-return of security $i$ over the period $t$ to $T$ conforms to the following single-factor model (also known as the CAPM that was presented in Sharpe (1964)):

$$R_i(t,T) = A_i(t,T) + B_i(t,T)R_F(t,T) + \epsilon_i(t,T) \qquad i = 1, ..., N \tag{2.18}$$

where $A_i(t,T)$ and $B_i(t,T)$ are constants, $R_F(t,T)$ is the log-return of factor F (the market portfolio in the case of CAPM) and $\epsilon_i(t,T)$ is the idiosyncratic component of security $i$'s return. Furthermore, assume that the expected value of $\epsilon_i(t,T)$ is zero under both the risk-neutral and real-world probability measures and is independent of $R_F(t,T)$. Under these assumptions Theorem 3a was found, which gives:

$$SKEW_i(t,T) = \Psi_i(t,T)SKEW_F(t,T) + \Upsilon_i(t,T)SKEW_\epsilon(t,T) \tag{2.19}$$

where $SKEW_\epsilon(t,T)$ is the skewness of $\epsilon$ and

$$\Psi_i(t,T) = \left(1 + \frac{e^{r(T-t)}V_\epsilon(t,T)}{B_i^2(t,T)[e^{r(T-t)}V_F(t,T) - \mu_F^2(t,T)]}\right)^{-3/2} \tag{2.20}$$

$$\Upsilon_i(t,T) = \left(1 + \frac{B_i^2(t,T)[e^{r(T-t)}V_F(t,T) - \mu_F^2(t,T)]}{e^{r(T-t)}V_\epsilon(t,T)}\right)^{-3/2} \tag{2.21}$$

$$\tag{2.22}$$

The derivation of this is shown in Appendix B.2. It is noted in the Bakshi *et al.* (2003) that since the unsystematic component, $\epsilon_i$, requires no alteration when moving between measures, the above skewness law (equation (2.19)) will be obeyed under both the risk-neutral and real world measures. However, $\Psi_n(t,T)$ and $\Upsilon_n(t,T)$ may need to be adjusted so that the different variance contracts (i.e. $V(t,T)$'s) and mean contracts (i.e. $\mu(t,T)$'s) represent the measure under consideration. This result can be exploited by estimating the scalar $b_n(t,T)$ under the real-world measure and then using it in the risk-neutral world to calculate the risk-neutral skewness of security $i$. This was done in Taylor (2014) where a single-stock was related to the market index in order to construct volatility smiles for single-stock futures options.

The above theory can be extended to situations where there are two independent systematic factors driving security returns. Specifically, the following multi-factor model is assumed:

$$R_i(t,T) = A_i(t,T) + B_i(t,T)R_F(t,T) + C_i(t,T)R_G(t,T) + \epsilon_i(t,T) \tag{2.23}$$

for some systematic factors $F$ and $G$. In addition, assume that $R_F(t,T), R_G(t,T)$ and $\epsilon_i(t,T)$ are all independent of each other. With this model, it is then shown that:

$$\begin{aligned} SKEW_i(t,T) =& \Psi_i(t,T)SKEW_F(t,T) + \Theta_i(t,T)SKEW_G(t,T) \\ &+ \Upsilon_i(t,T)SKEW_\epsilon(t,T) \end{aligned} \tag{2.24}$$

where

$$\Psi_i(t,T) = \left(1 + \frac{C_i^2(t,T)[e^{r(T-t)}V_G(t,T) - \mu_G^2(t,T)] + e^{r(T-t)}V_\epsilon(t,T)}{B_i^2(t,T)[e^{r(T-t)}V_F(t,T) - \mu_F^2(t,T)]}\right)^{3/2} \tag{2.25}$$

$$\Theta_i(t,T) = \left(1 + \frac{B_i^2(t,T)[e^{r(T-t)}V_F(t,T) - \mu_F^2(t,T)] + e^{r(T-t)}V_\epsilon(t,T)}{C_i^2(t,T)[e^{r(T-t)}V_G(t,T) - \mu_G^2(t,T)]}\right)^{3/2} \tag{2.26}$$

$$\Upsilon_i(t,T) = \left(1 + \frac{B_i^2(t,T)[e^{r(T-t)}V_F(t,T) - \mu_F^2(t,T)] + C_i^2(t,T)[e^{r(T-t)}V_G(t,T) - \mu_G^2(t,T)]}{e^{r(T-t)}V_\epsilon(t,T)}\right)^{3/2} \tag{2.27}$$

The similarities of equations (2.25), (2.26) and (2.27) to equations (2.22) and (2.21) are noted. These can be further extended to multi-factor models involving three or more independent systematic factors with a similar equation relating the skewness of the security with the skewness of the factors.

## 2.4 Theory and Ideas presented in Taylor (2014)

This section presents some ideas presented in Taylor (2014) which are of great importance to the methodology of this dissertation.

The market for single-stock futures options is relatively illiquid in South Africa, with implied volatility data concentrated around a moneyness of 1. However, the implied volatility data for options on the FTSE/JSE Top40 futures contract (the market futures contract) is more liquid both across strike and term. The aim of Taylor's paper was to produce an implied volatility smile for a particular single-stock futures contract. It made use of the theory developed in Bakshi *et al.* (2003) by relating the single-stock futures contract to the market futures contract.

The volatility smile for both the single-stock futures contract and the market index futures contract was assumed to take the following quadratic form:

$$\sigma(m) = am^2 + bm + c \tag{2.28}$$

The volatility smile for the market index futures contract was determined by minimising the squared error between the quadratic volatility smile and the implied

volatility data.

In order to calculate the contracts $V, W, X$ and $\mu$ (equations (2.10), (2.11), (2.12) and (2.9)) for the market, the moneyness range was discretised between the values 0 and 2 (this is detailed in the methodology of this dissertation in Section 3.1.1). The integrals in these equations were then numerically estimated over the discretised moneyness range. These contracts were subsequently used to determine the risk-neutral skewness of the market index futures contract, as given by equation (2.13).

The risk-neutral skewness of the single-stock futures contract was then found by using the CAPM relation of equation (2.18). Due to the rollover effect of futures contracts, the CAPM relationship was approximated by a regression of the actual single-stock returns against the actual market index returns. The results of this were then used in combination with the risk-neutral skewness of the market index futures contract to calculate the risk-neutral skewness of the single stock futures contract.

Taylor noted that equation (2.13) provided a "direct, but non-linear, relationship between the volatility smile and the risk-neutral skewness". This is because the risk-neutral skewness is determined by the contracts $V, W, X$ and $\mu$, and these all require put and call option prices over the strike range, i.e. a volatility smile. Consequently, an optimisation routine can be used to reverse the process and determine a volatility smile that corresponds to a particular risk-neutral skewness. This was done for the single-stock futures contracts along with the added constraint that the volatility smile must equal the observed implied volatility at-the-money (i.e. at a moneyness of 1), in the case where an observed implied volatility is available for the single-stock futures option contract.

# Chapter 3

# Methodology

This section details the methodology of constructing a volatility smile for a managed fund. This methodology can then be applied over different maturities in order to construct a volatility surface. The methodology makes use of the theory developed in Chapter 2. In addition, this methodology requires assuming the power utility function represents the preferences of the insurance company writing the investment guarantee, and that this is so for all assets. In particular, the insurance company is assumed to have the same relative risk aversion as that of the market.

The notation introduced in Section 2.1 will be used. Assume a managed fund, $MF$, which comprises $N$ assets with prices $S_t^{(1)}, ...S_t^{(N)}$ and a market index $M$ at time $t$. Moreover, the log-returns over the time period $t$ to $T$ are: $R_{MF}(t,T)$ for the managed fund, $R_M(t,T)$ for the market index and $R_i(t,T)$ for $i = 1, ..., N$.

## 3.1 Methodology Details

Consider the scenario where there is historical returns data for: a managed fund and all factors identified to have an influence on the return of the managed fund (e.g. constituent assets of the fund, benchmark assets of the fund or broad market indices). It is assumed these influential factors for the fund have already been identified. This is assumed as the methods used to identify such factors falls outside the focus of this dissertation. Moreover, assume a volatility surface of this managed fund is to be constructed as at some time $t$.

The methodology can be broken down into 3 main parts, which are explained in

the sections below. Firstly, the relative risk aversion parameter is estimated for the term under consideration in Section 3.1.1. Secondly, the volatility smile is determined for each influential factor as well as its risk-neutral skewness in Section 3.1.2. Thirdly, the risk-neutral skewness of the managed fund is calculated by relating the return of the fund to the influential factors in Section 3.1.3. Finally, the risk-neutral skewness of the managed fund is used to calculate the volatility smile of the managed fund for a particular term, which is also detailed in Section 3.1.3. Parts two and three, detailed in Sections 3.1.2 and 3.1.3, make use of an optimisation routine in order to determine the volatility smile for the given security.

A quadratic volatility smile in moneyness is used for all assets when implementing this method below, in Chapter 4. However, we could also use other functional forms, such as an exponential or spline, to represent the volatility smile. The methodology detailed below is for a generic volatility smile. Moreover, one functional form does not need to be assumed for all assets/factors, and a different functional form could be used for each asset/factor involved, if wanted.

### 3.1.1 Part 1: Estimating Relative Risk Aversion

Begin by assuming the power utility function represents the preferences of the market. Subsequently, estimate the relative risk aversion parameter, $\gamma(t, T)$, for a specific maturity. This is done by carrying out the following steps, where the asset under consideration is the market index:

1. Determine the continuous volatility smile of the asset:
   (a) Obtain implied volatilities for the market index and plot these points with respect to moneyness.
   (b) Assume a functional form for the implied volatility smile. Carry out a least squares procedure to fit this volatility smile to these points. A similar procedure was carried out in Beber (2001), Panayiotis *et al.* (2008), Taylor (2014) and Tompkins (2001) .
2. Calculate the risk-neutral skewness:

(a) Discretize the moneyness range into 2000 equally spaced points between 0.001 and 2, i.e. $0.1\% \leq m \leq 200\%$. Determine the implied volatilities, corresponding to the volatility smile (found above), at these points. Calculate 2000 option prices corresponding to these points where for $m < 1$ only out-of-the-money put option prices are used and for $0.999 < m$ only out-of-the-money call option prices are used.

This discretisation process is illustrated in the diagram below, where the number of discretisations is below the 2000 mentioned above for means of presentation.

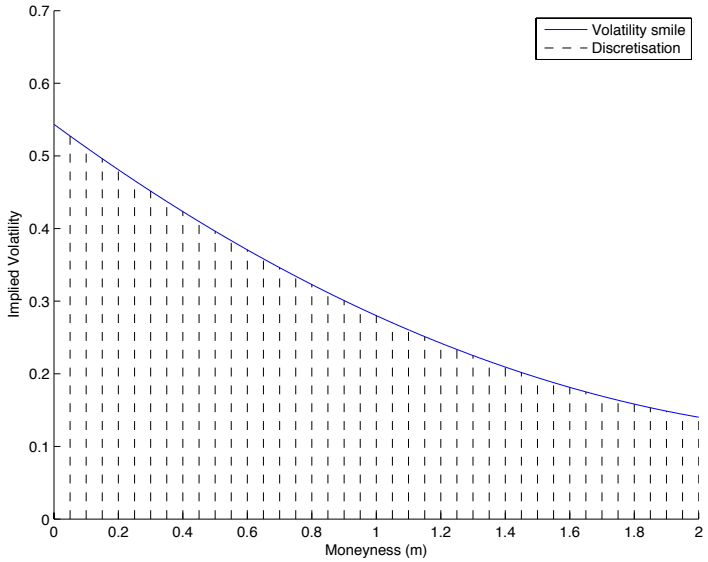


**Fig. 3.1:** Illustration of the discretisation of a fictitious volatility smile over the moneyness range of 0 to 2

(b) Approximate the integrals in equations (2.10), (2.11) and (2.12) by a finite sum over the 2000 option prices to calculate $V(t,T)$, $W(t,T)$ and

$X(t,T)$. So, for example, $V(t,T)$ will have the following form:

$$V(t,T) = \sum_{m=1}^{2} \frac{2\left(1 - \ln\left(\frac{K}{S_t}\right)\right)}{K^2} C\big(t,T;\sigma(m)\big)\,(0.001) + \sum_{m=0}^{0.999} \frac{2\left(1 - \ln\left(\frac{K}{S_t}\right)\right)}{K^2} P\big(t,T;\sigma(m)\big)\,(0.001)$$

In the equation above, the 0.001 term involved in the summations is as a result of discretising the moneyness range such that each discrete point is a moneyness of 0.001 apart.

(c) Use $V(t,T)$, $W(t,T)$ and $X(t,T)$ to calculate $\mu(t,T)$ (i.e. equation (2.9)). Consequently, use these to calculate the $(T-t)$ period risk-neutral skewness given by equation (2.13):

$$SKEW(t,T) = \frac{e^{r(T-t)}\Big[W(t,T) - 3\mu(t,T)V(t,T)\Big] + 2\big(\mu(t,T)\big)^3}{\Big\{e^{r(T-t)}V(t,T) - \big(\mu(t,T)\big)^2\Big\}^{\frac{3}{2}}}$$

3. Determine real-world moments

(a) Using historical data, produce a time series of overlapping $(T-t)$ log-returns, as done in Taylor (2014). For example, if 5 years of daily log-returns are available and yearly log-returns are required, overlapping annual log-returns are produced starting from the first day of the second year. This will give the log-return from the first day of the first year to the first day of the second year. The next data point will be the yearly log-return from the second day of the first year to the second day of the second year and so on. This is also known as rolling data points. In this example, 4 years worth of 1-year overlapping returns would result. Produce 1000 such points (or as many as possible, up to time $t$).

(b) From this series, calculate the real-world sample standard deviation, skewness and kurtosis. This approach is carried out in order to have enough data to obtain meaningful estimates. In addition, this approach

may capture the characteristics of the $(T-t)$ log-returns which may be lost or distorted if daily returns were scaled up to $(T-t)$ period returns. It is noted in Cont (2001) how asset return distributions are different for different time horizons.

4. Use the risk-neutral skewness and the real-world moments of the market index to solve for $\gamma(t,T)$ in equation (2.17):

$$SKEW(t,T) \approx \overline{SKEW}(t,T) - \gamma(t,T)\left(\overline{KURT}(t,T) - 3\right)\overline{STD}(t,T)$$

It is important to note that this estimate is for a specific time horizon. In addition, it is noted that this equation above is only an approximation and thus this step will provide an approximation of $\gamma(t,T)$.

### 3.1.2 Part 2: Determining Volatility Smile and Risk-Neutral Skewness of an Influential Factor

The following steps are carried out in order to determine the volatility smile and risk-neutral skewness of each influential factor:

1. Carry out steps 1 and 2 in Section 3.1.1 for all influential factors that have a quoted options market. This will give the fitted volatility smile and risk-neutral skewness for all such influential factors.

2. Calculate the risk-neutral skewness for influential factors that do not have a quoted options market:

   (a) In the same way as in Section 3.1.1, construct a time series of overlapping $(T-t)$ log-returns for the influential factor consisting of 1000 points, up to time $t$. From this series, estimate its real-world standard deviation, skewness and kurtosis.

   (b) Use the estimate of $\gamma(t,T)$, from Section 3.1.1, and the real-world moments of the influential factor to calculate its risk-neutral skewness as

given by equation (2.17):

$$SKEW(t,T) \approx \overline{SKEW}(t,T) - \gamma(t,T)\left(\overline{KURT}(t,T) - 3\right)$$

3. Determine the volatility smile for the influential factors that do not have a quoted options market:

   (a) Discretise the moneyness range into 2000 equally spaced points as done in Section 3.1.1. Apply this discretisation to the integrals needed to determine $V, W$ and $X$ in equations (2.10), (2.11) and (2.12).

   (b) Assume a functional form for the volatility smile, $\sigma(m)$, and substitute this into the discretised integrals of equations (2.10), (2.11) and (2.12).

   (c) Use (2.13) to find the functional form of the $(T-t)$-period risk-neutral skewness, $SKEW(t,T)$, in terms of the volatility smile function parameters. Thus:

$$SKEW(t,T) = \frac{e^{r(T-t)}\Big[W(t,T) - 3\mu(t,T)V(t,T)\Big] + 2\big(\mu(t,T)\big)^3}{\Big\{e^{r(T-t)}V(t,T) - \big(\mu(t,T)\big)^2\Big\}^{\frac{3}{2}}}$$

   where $V, W$ and $X$ (in equations (2.10), (2.11) and (2.12)) have as inputs put and call option prices over the strike range. Furthermore, put and call option prices, for a particular strike price, have as an input the BSM implied volatility, for that particular strike price.

   (d) Use the Nelder-Mead downhill simplex method to determine the optimal parameters for the volatility smile that minimises the absolute error between the output risk-neutral skewness of equation (2.13) and the skewness calculated in step 2 above. Consequently, the objective function to be minimised will be:

$$\left| \frac{e^{r(T-t)}\Big[W(t,T) - 3\mu(t,T)V(t,T)\Big] + 2\big(\mu(t,T)\big)^3}{\Big\{e^{r(T-t)}V(t,T) - \big(\mu(t,T)\big)^2\Big\}^{\frac{3}{2}}} - SKEW(t,T) \right|$$

Thus the optimisation routine determines the volatility smile for the asset that optimally corresponds to its risk-neutral skewness. If a quadratic function, as given in equation (2.28), is assumed for the volatility smile then there are three unknowns which the optimisation procedure solves for, namely $a$, $b$ and $c$ in equation (2.28). The optimal parameters will then produce a volatility smile, which corresponds to a risk-neutral skewness value (when the volatility smile is input into equation (2.13) ) that is minimally different to its risk-neutral skewness (calculated in step 3c above).

In order for this to give sensible results, constraints may need to be imposed on the output volatility smile. This will depend on the characteristics of the asset under consideration as well as available data on this asset. For example, in Taylor (2014) the volatility smile was constrained to pass through market quoted at-the-money implied volatilities, if available.

Furthermore, the optimisation routine requires starting values, which correspond to a set of initial volatility smile parameters, in order for the routine to be carried out. These starting values should correspond to a sensible volatility smile for this particular asset to ensure the output is sensible. This is because the volatility smile that results from the optimisation routine is often similar to the initial volatility smile (i.e. the starting values) supplied to the optimisation routine. These starting values could be those of a similar asset in a similar market. However, the more constraints that are placed on the resultant volatility smile, the less affect the starting values have on the output volatility smile.

### 3.1.3 Part 3: Calculating the Risk-Neutral Skewness and Volatility Smile of a Managed Fund

The risk-neutral skewness of a managed fund is now calculated. In order to do this the volatility smile and risk-neutral skewness are required for each influential factor, as determined in the above sections. For ease of exposition, assume there

are two influential factors for this managed fund. However this method can easily be extended to incorporate a larger number of influential factors by extending the results of Section 2.3.3.

The following steps are carried out:

1. Assume a two-factor linear model, as given by equation (2.23), holds. Here the log-return of the managed fund is driven by the log-return of the influential factors, as shown by:

$$R_{MF}(t,T) = A_{MF}(t,T) + B_{MF}(t,T)R_1(t,T) + C_{MF}(t,T)R_2(t,T) + \epsilon_{MF}(t,T)$$

Recall that it is assumed the influential factors are independent. This can be a limiting assumption as often the factors influencing the returns of a fund may not be independent.

2. Construct a time series of overlapping $(T-t)$ log-returns for the fund in the same way as done in Section 3.1.1

3. Perform an ordinary least squares regression of the fund's $(T-t)$ log-returns against the two corresponding log-returns of the influential factors. This is done in order to estimate the coefficients $B_{MF}$, $C_{MF}$ and the variance of the residuals of the two-factor model. These are then used to calculate the coefficients $\Psi_{MF}(t,T), \Theta_{MF}(t,T)$ and $\Upsilon_{MF}(t,T)$ as given in equations (2.25), (2.26) and (2.27).

4. Use the risk-neutral skewness values for the influential factors and the coefficients calculated above to calculate the risk-neutral skewness for the fund using equation (2.24):

$$\begin{aligned} SKEW_{MF}(t,T) =& \Psi_{MF}(t,T)SKEW_1(t,T) + \Theta_{MF}(t,T)SKEW_2(t,T) \\ &+ \Upsilon_{MF}(t,T)SKEW_\epsilon(t,T) \end{aligned}$$

5. Assume a functional form for the volatility smile of the managed fund. Carry out the same procedure detailed in Section 3.1.2 step 3 for the managed fund.

This results in a volatility smile for the managed fund for the maturity considered. Note that this methodology easily extends to funds comprising more than two assets by simply extending equation (2.23) to include more independent factors.

## 3.2 Methodology: Possible Difficulties

In this section some of the difficulties that may be encountered in practice when trying to implement the above methodology are confronted.

One such difficulty is that the influential factors identified to effect the return of a fund may not be independent. This means the results from Section 2.3.3 cannot be applied as independent factors are needed. In this case, it is suggested that the fund be related to a minimal number of influential factors, which showcase a low correlation with one another. Furthermore, a principal components analysis could be carried out to obtain a number of statistically orthogonal factors, which are a linear combination of the original factors. For more detail relating to principal components analysis of financial data, see Alexander (2001). An attempt could then be made to use these in the above methodology, specifically in Section 3.1.2. However, this requires further work to investigate whether this is viable and how it would be applied, which falls outside the scope of this dissertation.

The problem above will also be encountered when letting each constituent asset of the managed fund be an influential factor. This is the case as managed funds are often made up of many assets which are usually not independent. This is the reason for presenting the above methodology in the context of having a few influential factors, which display reasonable independence.

A third difficulty arises when there is a managed fund where the constituent asset weightings in the fund change dramatically over the life of the fund. In this instance, one solution may be the construction of synthetic fund data. In other words, historical synthetic fund data could be constructed by letting each constituent asset contribute to the return of the fund according to its current weighing. This will require an assumption regarding how often the fund constituents would be altered to correct any changes in their relative weights as well as transaction costs incurred

to carry out these re-weightings. This synthetic fund data can then be treated as the fund in the above methodology. This should then produce a volatility surface which better represents the current composition of the fund.

# Chapter 4

# Empirical Tests and Results

In this section the theory and methodology developed in earlier chapters is applied in a practical South African setting.

To begin, the relative risk aversion of different markets is estimated in Section 4.1 by assuming the power utility function represents the preferences of the markets. This allows the methodology of Section 3.1 to be applied to a fictitious managed fund in order to determine volatility smiles at three different maturities for this fund, which is done in Section 4.2 below. This fictitious fund is constructed to consist of an equity element, represented by the JSE/FTSE Top40 Total Return Index, and a fixed interest element, represented by the All Bond Total Return Index

## 4.1 Data

In the following sections of this chapter, quoted index data and implied volatilities of these indices, if available, are used.

Specific use is made of the following index data obtained from Bloomberg: the index series for the FTSE/JSE Top40 Index (Top40), S&P500 Index (S&P500), JSE Top40 Total Return Index (Top40 TR) and Total Return All Bond Index (ALBI TR). For the Top40 and S&P500, index values from 02/01/1996 to 12/12/2013 are used. This corresponds to 4490 points for the Top40 and 4520 points for the S&P500, which are different due to the different number of trading days in the different markets. These points are used to construct log-returns series of different maturities, in the manner described in Section 3.1.1 point 3(a), from the 02/01/1997 to 12/12/2013.

The index points for the Top40 TR and ALBI TR are used from 03/01/2006 to 18/12/2012 in order to construct a fictitious fund. It is noted that these indices are not traded, however they were chosen since they provide a good example of what a managed fund would broadly be made up of. These index points are filtered so that only days where both indices are quoted are used. This corresponds to 1735 index points each. In the same way as above, these index points are used to construct log-returns series of different maturities from the 02/01/2007 to 18/12/2012.

In addition, discrete implied volatility points for the FTSE/JSE Top40 Futures Index and the S&P500 Index are used. These were obtained from Old Mutual Specialised Finance (OMSFIN), who obtained the data from a South African broker, and Bloomberg respectively. These implied volatilities were collected for maturities of 3 months, 6 months and 1 year, as at the following dates: 19 March, 18 June, 17 September and 18 December 2012. The implied volatilities for the FTSE/JSE Top40 Futures Index correspond to discrete moneyness points from 75% to 125% in 1% increments, in other words implied volatilities for 51 different strike prices. It must be noted that fewer strike prices are actually available in the market and so this implies that the broker would have carried out some form of interpolation method. This must be borne in mind when interpreting the results, however this should not be too influential as it is expected that the general shape and slope of the volatility smile (just made up of market data) before interpolation will be similar to that of the volatility smile after interpolation is carried out. The implied volatilities for the S&P500 Index correspond to discrete moneyness points of 60%, 90%, 95%, 97.5%, 100%, 102.5%, 105%, 110%, 120%, 150% and 200%

It is noted that convention in the South African futures options market is to quote implied volatilities that correspond to a traded price when the risk-free rate and dividend yield are set to zero. Consequently, when a futures contract underlies an option in the South African market, the risk-free rate, $r$, and the dividend yield, $q$, are set to zero when calculating the price, as given by equations (2.1) and (2.2). This is because the futures price already accounts for the carry cost. In other words, if the underlying index has a spot price of $S$, then the futures price, $F$, with term $t$ is $F = Se^{(r-q)t}$, which cancels out with the $r$ and $q$ terms when substituted into

equations (2.1) and (2.2). When dealing with a total return index as the underlying asset, the dividend yield, $q$, is set to zero when calculating option prices.

## 4.2 Estimating Relative Risk Aversion

Bakshi *et al.* (2003) assumed the power utility function in wealth and then used equation (2.17) to estimate the coefficient of relative risk aversion, $\gamma$, for options written on the S&P100 index with maturities of 58 and 86 days.

This work similarly looks at estimating $\gamma$ for different time horizons in order to assess the reasonability of the methodology of Section 3.1.1. Two markets are considered with the power utility assumption. The S&P500 Index and the FTSE/JSE Top40 Index Futures along with their corresponding option markets are used to estimate $\gamma$ for different time horizons.

In order to do this, a functional form must be assumed for the implied volatility smile. A popular deterministic function in the literature is the quadratic function, which characterises many markets around the world, particularly equity markets (see Beber (2001), Homescu (2011), Kotzé and Joseph (2009), Kotzé *et al.* (2013), Panayiotis *et al.* (2008), Peña *et al.* (1999), Taylor (2014) and Tompkins (2001)). It is noted in Dumas *et al.* (1998) that Black-Scholes implied volatilities often have a parabolic shape. In addition, the use of quadratic volatility functions is substantiated in Dumas *et al.* (1998) by arguing that prices far from the current price have probability weights that become very small at a rapid rate. This is used as justification in Dumas *et al.* (1998) for fitting quadratic functions to local volatility smiles based on the S&P500. Furthermore, there have been a number of principle component analyses carried out on implied volatility smiles, which found evidence supporting the use of quadratic functions (see Kotzé and Joseph (2009) for a summary). Lastly, it was found in Kotzé and Joseph (2009) that quadratic volatility functions were the best models to calibrate volatility surfaces for the South African option market and since all investigations in this dissertation will be carried out in a South African context, this functional form is assumed for all implied volatility functions.

Before moving on it must be mentioned that the FTSE/JSE Top40 Futures mature on the third Thursday of March, June, September and December every year. Exchange traded options based on the FTSE/JSE Top40 Futures contracts also expire on the same dates. However, the Futures close out process is facilitated through a 15 minute auction call session which starts at 12:00 in the underlying equity Spot market. If the instrument does not trade during this auction session, the reference price will be used. The reference price is either the last trade for the current day or the previous close. Thus, the final price of the Futures contract on these dates is unlikely to be exactly the same as the closing FTSE/JSE Top40 Index value for the day, but they should be relatively close given that the time delay between the two being determined is relatively short. Consequently, as an approximation, when carrying out the estimation of the moments for the FTSE/JSE futures contract, use is made of the FTSE/JSE Top40 Index in order for there to be enough data to acquire reasonable estimates, as done in Taylor (2014). However, for the S&P500 options the underlying instrument is the index itself and so the real-world moments are estimated from its log-returns series.

| **FTSE/JSE Top40** | | | | **S&P500** | | | |
|---|---|---|---|---|---|---|---|
| Maturity | Kurtosis | Skewness | Std | Maturity | Kurtosis | Skewness | Std |
| 1Y | 3.62 | -0.80 | 0.20 | 1Y | 4.01 | -1.07 | 0.19 |
| 6M | 4.55 | -1.08 | 0.15 | 6M | 6.11 | -1.28 | 0.13 |
| 3M | 4.68 | -0.89 | 0.11 | 3M | 6.63 | -1.25 | 0.08 |

**Tab. 4.1:** FTSE/JSE Top40 Index and S&P500 Index real-world moments for different maturities using rolling returns from 02/01/1997 to 12/12/2013

The real-world moment estimates are shown in Table 4.1. It appears that for all three time horizons, the S&P500 index displays greater real-world kurtosis and more negative skewness for this particular period considered. In addition, it seems the Top40 Index and S&P500 Index have similar real-world volatility levels (in this case the standard deviation of real-world log-returns). So for the same coefficient of relative risk aversion, $\gamma$, in equation (2.17) we would expect the S&P500 index

to display a more negative risk-neutral skewness. However, as seen in Table 4.2 the different markets display different coefficients of relative risk aversion for different maturities.

The steps presented in Section 3.1.1 are now applied in order to estimate the relative risk aversion for both the FTSE/Top 40 Index Futures contract and the S&P500 Index. This is done for the maturities of 3 months, 6 months and 1 year as at March, June, September and December in the year 2012. Approximately mid-month data for the Top40 futures options is used in order to have maturities that closely match 3 months, 6 months and 1 year.

An example of the volatility smiles fitted to market data for a maturity of 1 year is shown below in Figures 4.1 and 4.2. See Figures C.1, C.2, C.5 and C.6 for the volatility smiles for the maturities of 3 months and 6 months in Appendix C.1. Figure 4.1 shows the 1-year smiles for the FTSE/JSE Top40 Futures Index and 4.2 for the S&P500 Index, where the dots represent market data.

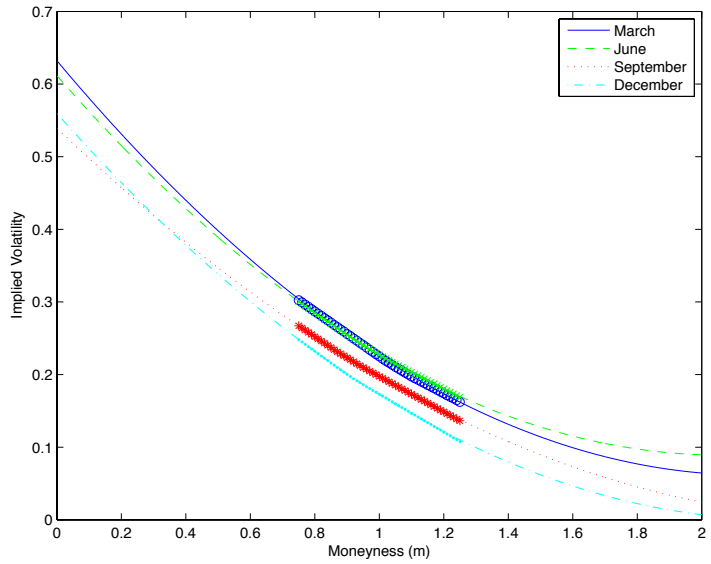


**Fig. 4.1:** FTSE/JSE Top40 1-year quadratic volatility smiles for the year 2012 as at March 19, June 18, September 17 and December 18

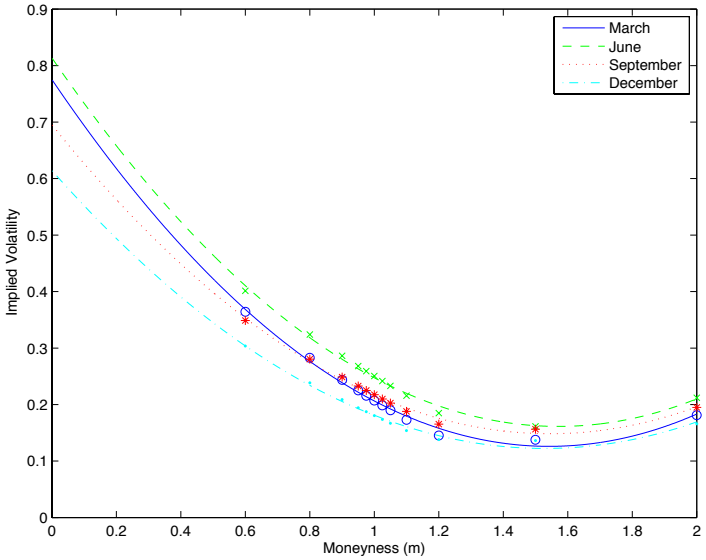


**Fig. 4.2:** S&P500 1-year quadratic volatility smiles for the year 2012 as at March 19, June 18, September 17 and December 18

After fitting each volatility smile, the risk-neutral skewness is estimated before estimating the coefficient of relative risk aversion, $\gamma$. The risk-neutral skewness along with the corresponding estimate of $\gamma$, for the different months considered in the year 2012 are displayed in Table 4.2. Since the real-world moments were confined to remain the same over the different months considered, the estimates of $\gamma$ differ solely due to the different risk-neutral skewness estimated from the volatility smiles. Consequently, when the risk-neutral (RN) skewness is more negative, it results in a higher estimate of $\gamma$.

| | | FTSE/JSE Top40 | | S&P500 | |
|---|---|---|---|---|---|
| Maturity | Month | RN Skewness | $\gamma$ | RN Skewness | $\gamma$ |
| **1Y** | mar | -2.10 | 10.28 | -3.08 | 10.27 |
| | jun | -1.92 | 8.86 | -2.74 | 8.53 |
| | sep | -1.83 | 8.16 | -2.36 | 6.59 |
| | dec | -2.21 | 11.19 | -2.16 | 5.55 |
| **6M** | mar | -1.86 | 3.28 | -3.45 | 5.49 |
| | jun | -2.03 | 3.98 | -2.92 | 4.13 |
| | sep | -1.91 | 3.49 | -2.55 | 3.21 |
| | dec | -1.70 | 2.63 | -1.91 | 1.61 |
| **3M** | mar | -1.57 | 3.69 | -2.41 | 3.87 |
| | jun | -1.95 | 5.78 | -2.27 | 3.39 |
| | sep | -1.26 | 2.04 | -1.49 | 0.82 |
| | dec | -0.98 | 0.50 | -1.05 | -0.65 |

**Tab. 4.2:** FTSE/JSE Top40 and S&P500 Index Risk-Neutral (RN) Skewness and $\gamma$ estimates as at March 19, June 18, September 17 and December 18 in the year 2012

Table 4.2 shows estimates of $\gamma$ for the FTSE/JSE Top40 to generally be greater than the corresponding ones for the S&P500. This may be due to South Africa being an emerging market, which may have a higher fear factor associated with it. Issler and Piqueira (2000) similarly found the coefficient of relative risk aversion to be higher for the emerging market of Brazil compared to that of America. From Table 4.2, it seems that $\gamma$ increases as the maturity increases, although this is more so for the American market. Intuitively this makes sense: the market becomes more risk averse as the considered time period increases since there is usually increased uncertainty accompanied with time horizons further in the future. The results obtained here fall broadly in line with those found in Bakshi *et al.* (2003), Bliss and Panigirtzoglou (2004), Ferson and Constantinides (1991) and Issler and Piqueira

(2000).

## 4.3 Constructing a Volatility Surface for a Managed Fund

In this section the methodology outlined in Section 3.1 is applied in order to construct a volatility surface for a fictitious managed fund. This is done by constructing volatility smiles for the maturities of 3 months, 6 months and 1 year as at 18 December 2012. These maturities are considered due to the limited amount of data in South Africa, which is especially the case for maturities greater than 1 year.

A managed fund comprising the JSE Top40 Total Return (Top40 TR) index and the All Bond Total Return Index (ALBI TR) is created. This fund is examined from 03/01/2006 to 18/12/2012 where the fund is initially invested 60% in the Top40 TR index and 40% in the ALBI TR index. Every 3 months it is rebalanced into the same constituent weights, where it is assumed there are no transaction costs. Daily overlapping 3-month, 6-month and 1-year rolling returns series are then constructed from 02/01/2007 to 18/12/2012 for each of the constituents and the fund. Furthermore, the Top40 TR index and the ALBI TR index will be treated as the influential factors for this managed fund.

The relative risk aversion estimates for the FTSE/JSE Top40 Futures Index, as at 18 December 2012, are applied to calculate the volatility smiles of the influential factors. This basically involves performing the steps outlined in Section 3.1.1 for the FTSE/JSE Top40 Futures Index, as done in the previous section. The steps in Section 3.1.2 are then performed to determine risk-neutral skewness and the volatility smile for the Top40 TR and the ALBI TR. Subsequently, the steps in Section 3.1.2 are performed to determine the risk-neutral skewness and volatility smile for the fund. This involves assuming the following two-factor linear returns model:

$$R_{MF}(t,T) = A_{MF}(t,T) + B_{MF}(t,T)R_{T40}(t,T) + C_{MF}(t,T)R_{ALBI}(t,T) + \epsilon_{MF}(t,T)$$

where $R_{MF}$, $R_{T40}$ and $R_{ALBI}$ are the log-returns of the managed fund, the Top40 TR and the ALBI TR respectively. Note that by using this model it is assumed that the Top40 TR and ALBI TR are independent.

The regression estimates for the coefficients of this two-factor linear returns model, for different maturities, is shown below in Table 4.3.

| | $A(t,T)$ | $B(t,T)$ | $C(t,T)$ | R-squared |
|---|---|---|---|---|
| 1Y | -0.031 | 0.612 | 0.664 | 0.811 |
| 6M | -0.013 | 0.709 | 0.501 | 0.763 |
| 3M | -0.005 | 0.760 | 0.401 | 0.766 |

**Tab. 4.3:** Two factor linear model coefficient regression estimates for the fictitious managed fund comprising of the JSE Top40 TR Index and the ALBI TR Index for different maturities over the period 02/01/2007 to 18/12/2012 along with the associated R-squared for each model

It must be noted that these estimates differ from the original 60:40 split since we must deal with log-returns and not absolute returns when making use of the above theory.

The real-world and risk-neutral moments for each influential factor and the fund are shown below in Table 4.4.

| Maturity | Asset | Real-world | | | Risk-neutral |
|---|---|---|---|---|---|
| | | Kurtosis | Skewness | Std | Skewness |
| **1Y** | Top40 TR | 3.81 | -1.18 | 0.21 | -3.09 |
| | ALBI TR | 2.84 | -0.53 | 0.05 | -0.44 |
| | Fund | 4.15 | -0.99 | 0.14 | -1.46 |
| **6M** | Top40 TR | 6.43 | -1.69 | 0.16 | -3.08 |
| | ALBI TR | 4.23 | 0.29 | 0.05 | 0.14 |
| | Fund | 6.17 | -1.32 | 0.12 | -2.06 |
| **3M** | Top40 TR | 5.94 | -1.44 | 0.10 | -1.58 |
| | ALBI TR | 3.17 | 0.32 | 0.03 | 0.31 |
| | Fund | 5.14 | -1.00 | 0.09 | -0.78 |

**Tab. 4.4:** Real world and risk-neutral central moment estimates for the Top40 TR Index, ALBI TR Index and the Managed Fund as at the 20 December 2012

The above table shows how the real-world standard deviation of log returns (Std) decreases when the ALBI TR asset is combined with the Top40 TR asset. It also shows that the risk-neutral skewness for the fund is always lower than that of the Top40 TR.

When carrying out the steps in Sections 3.1.2 and 3.1.3, the optimisation output was found to be very sensitive to the starting values which were provided to the optimisation routine. Consequently, the fitted volatility smile parameters for the FTSE/JSE Top40 Futures Index were chosen as the starting values for the optimisation routine that calculates the volatility smile for the Top40 TR. For the ALBI TR a flat smile, equal to the ALBI TR historical volatility, was supplied for the starting values in this case. When using the optimisation routine to determine the volatility smile for the managed fund, the starting parameter values which were supplied corresponded to a smile that is 60% of the Top40 TR volatility smile. This provided the optimisation routine with feasible parameters for the volatility smile of

the fund. The fund volatility smile was also constrained to lie below the volatility smile of the Top40 TR at a moneyness of 1, since the volatility smile of the fund is expected to be below that of its equity component. This is expected because the equity component of managed funds is usually its most volatile component, as is the case for this fictitious managed fund. In addition, the effect of diversification between different asset classes results in the actual realised volatility of the fund to be between the realised volatility of its most volatile constituent and its least volatile constituent.

An example of the volatility smiles for the influential factors and the fund are shown in Figure 4.3 below for the maturity of 1 year. The corresponding volatility smiles for the maturities of 6 months and 3 months can be found in Appendix C.2 in Figures C.5 and C.6.

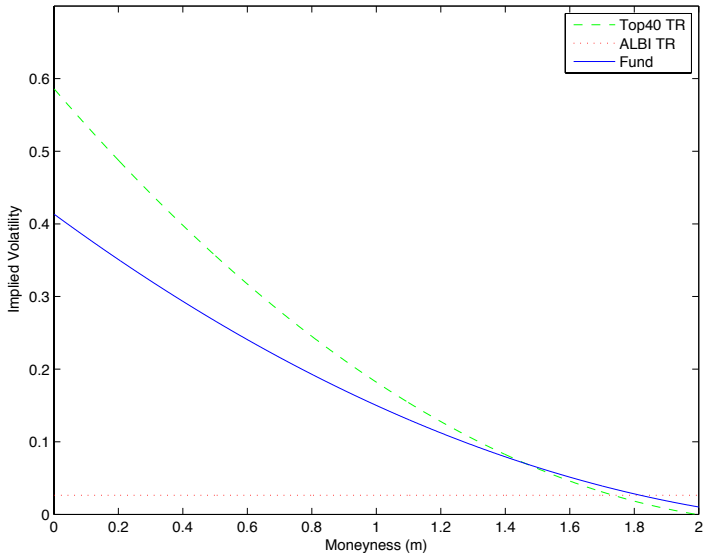


**Fig. 4.3:** Volatility smiles of Top40 TR, ALBI TR and the ficticious managed fund as at 18 December 2012 for a maturity of 1 year

One of the problems with the above methodology is that there are no points on which to pin down the volatility smile of the fund. This is in contrast to what was done in Taylor (2014) where at minimum, there were at-the-money implied volatil-

ities to pin down the volatility smile for single-stock futures options. In this work, it was noted that most at-the-money implied volatilities are similar to the historical volatilities observed for the particular asset. Consequently all fund volatility smiles were constrained to fall within 5% of the fund's historical volatility, for that specific time horizon.

The final result consists of the volatility smiles for the fund for the 3 maturities considered. This is shown in Figure 4.4 below.

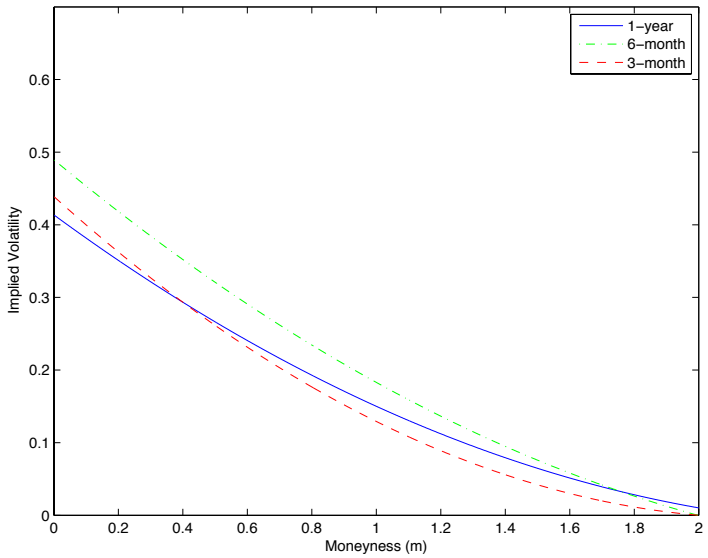


**Fig. 4.4:** Fictitious managed fund quadratic volatility smiles as at 20/12/2012 for maturities of 3 months, 6 months and 1 year

Theoretically, the methods utilised herein can be carried out for more maturities, which can then be combined to provide a surface.

According to Figure 4.4, the 6-month volatility smile appears to be the most negatively sloped. It also has the largest negative risk-neutral skewness, which is -2.06. The 3-month and 1-year volatility smiles have similar negative slopes, while their risk-neutral skewness are relatively different. For the ALBI TR it is seen, in Table 4.4, that it has a risk-neutral skewness that is generally positive and also has relatively flat or upward sloping volatility smiles, as shown in Figures

4.3, C.5 and C.6. These results thus generally fall in line with those observed in Bakshi *et al.* (2003), where more negatively sloped volatility smiles correspond to distributions with more negative risk-neutral skewness. The impact of constraining the resulting volatility smiles influences the degree to which they are able to be negatively sloped and is thus one reason why there is not a clear-cut relationship between the magnitudes of the slope and the risk-neutral skewness for this managed fund.

# Chapter 5

# Conclusion

When constructing a volatility surface for a managed fund the methodology presented in this dissertation is just one of many possible alternatives. Furthermore, the methodology contained herein could itself be modified in a variety of ways. In particular, the methodology could be modified by:

- Changing the way the moments of the real-world log-return distribution of assets are estimated
- Making use of a different utility function
- Assuming a different functional form for the volatility smile function (such as an exponential or spline)
- Making use of a different optimisation routine
- Adding additional logical constraints to the optimisation output (depending on the assets involved)

There are also many other possible modifications or additions that could be made.In addition, some of the ideas discussed in Section 3.2 could also be adopted.

Alternative ideas for constructing a volatility surface for a managed fund may be developed from the ideas presented in de Araújo and Maré (2006) and Flint *et al.* (2012). These focus on historical risk-neutral return distributions, which are derived from real-world historical returns series that are adjusted so that the expectation coincides with that of the risk-free rate. Once the risk-neutral return distribution is found, Monte Carlo simulation is used to price options. This could be done for

different strike prices to produce a volatility smile, and then repeated to produce multiple volatility smiles to construct a volatility surface.

In this dissertation an economically and mathematically sound methodology for constructing a volatility surface for a managed fund is presented. The volatility surface of the fund can be used to calibrate stochastic models, as mentioned in Chapter 1, which may be used in combination with Monte Carlo simulations to price and hedge guarantees (i.e. derivatives) based on the fund.

There are a few limitations concerning the methodology presented in this dissertation. To begin, equation (2.17) is only an approximation and as such it can be a source of variability, especially since it is used in both Sections 3.1.1 and 3.1.2 of the methodology. The methodology estimates $\gamma(t, T)$ based on a broad market index and then applies this to influential factors (which usually are assets or indices). This requires the assumption, that the $\gamma$ estimated from the market applies to these influential factors, is valid.

In addition, when relating a managed fund to its influential factors, use is made of linear factor return models, such as that shown in equation (2.23). One of the assumptions of this model is that the factors are independent. This may be an unrealistic assumption if a managed fund is related to many influential factors, such as all of its individual constituents. It is recommended that an attempt is made to relate a managed fund to a few influential factors which have evidence of being independent, or at least are less correlated. If this attempt does not resolve the issue, one possible route to get around this may be to carry out a principal components analysis and obtain a number of statistically orthogonal factors, which are a linear combination of the original factors. However, this requires further work to investigate whether this is viable and how it would be applied, which falls outside the scope of this dissertation.

Another limitation concerning the methodology presented in this dissertation is the accuracy of the method used to estimate the real-world moments. This makes use of over-lapping historical returns data, which may influence the resulting estimates of the moments. More sophisticated statistical methods for estimating these real-world moments may prove more accurate and give more credibility to the ideas presented

in this dissertation.

Finally, the optimisation routine used in this dissertation is sensitive to the starting values supplied to it when optimising over the three quadratic parameters of the volatility smile. Coupled with this, is the problem of not knowing a single point along the volatility smile of a managed fund and thus having no point at which to position it. This can result in unanticipated volatility smiles. In order to counteract these problems it is recommend that volatility smiles for similar assets be applied as possible starting values. Examination of historical volatilities for the managed fund may also help provide indications of roughly where the volatility smile is expected to be.

When pricing and hedging investment guarantees, it is important that the volatility smile used to calibrate stochastic models, is not unstable (i.e. arbitrary tweaks to the method should not yield huge changes in output). To improve stability a number of practical (or reasonable) restrictions can be imposed to improve the stability of the output. In addition these restrictions will ensure the output complies with specific boundaries or expectations that are believed to be reasonable.

# Bibliography


Alexander, C. (2001). *Market Models: A Guide to Financial Data Analysis*, John Wiley and Sons, Chichester.

Bakshi, G., Kapadia, N. and Madan, D. (2003). Stock return characteristics, skew laws, and the differential pricing of individual equity options, *Review of Financial Studies* **16**(1): 101–143.

Bakshi, G. and Madan, D. (2000). Spanning and derivative-security valuation, *Journal of Financial Economics* **55**(2): 205 – 238.

Beber, A. (2001). Determinants of the implied volatility function on the italian stock market.

Bingham, N. and Rudiger, K. (2004). *Risk-Neutral Valuation: Pricing and Hedging of Financial Derivatives*, 2 edn, New York, NY: Springer.

Bjork, T. (2009). *Arbitrage Theory in Continous Time*, 3 edn, Oxford University Press.

Black, F. and Scholes, M. (1973). The pricing of options and corporate liabilities, *Journal of Political Economy* **81**(3): pp. 637–654.

Bliss, R. R. and Panigirtzoglou, N. (2004). Option-implied risk aversion estimates, *The Journal of Finance* **59**(1): 407–446.

Cont, R. (2001). Empirical properties of asset returns: stylized facts and statistical issues, *Quantitative Finance* **1**(2): 223–236.

de Araújo, M. and Maré, E. (2006). Examining the volatility skew in the South African equity market using risk-neutral historical distributions, *Investment Analysts Journal* **64**: 15–20.

Deelstra, G., Grasselli, M. and Koehl, P. (2004). Optimal design of the guarantee for defined contribution funds, *Journal of Economic Dynamics and Control* **28**(11): 2239 – 2260.

Dennis, P. and Mayhew, S. (2002). Risk-neutral skewness: Evidence from stock options, *Journal of Financial and Quantitative Analysis* **37**: 471–493.

Derman, E., Kani, I. and Zou, J. Z. (1996). The local volatility surface: Unlocking the information in index option prices, *Financial Analysts Journal* **52**(4): pp. 25–36.
**URL:** *http://www.jstor.org/stable/4479931*

Dumas, B., Fleming, J. and Whaley, R. E. (1998). Implied volatility functions: Empirical tests, *The Journal of Finance* **53**(6): 2059–2106.

Ferson, W. E. and Constantinides, G. M. (1991). Habit persistence and durability in aggregate consumption: Empirical tests, *Journal of Financial Economics* **29**(2): 199 – 240.

Flint, E., Chikurunhe, F. and Seymour, A. (2012). (Un)Modelling the Volatility Surface: Valuing South African Volatility Surfaces via Risk-Neutral Historic Return Distributions, *Technical report*, Peregrine Securities.

Greenbaum, M. and Ravindran, K. (2002). Dynamic hedging, *Record of the Society of Actuaries* **27**(1).

Hagan, P. S., Kumar, D., Lesniewski, A. S. and Woodward, D. E. (2003). Managing smile risk, *Wilmott Magazine (2003).* p. 249.

Hardy, M. (2003). *Investment guarantees: modeling and risk management for equity-linked life insurance*, Vol. 215, John Wiley & Sons.

Heston, S. (1993). A closed-form solution for options with stochastic volatility with applications to bond and currency options, *Review of Financial Studies* **6**(2): 327–343.

Homescu, C. (2011). Implied volatility surface: Construction methodologies and characteristics. Working Paper.
**URL:** *SSRN: http://ssrn.com/abstract=1882567*

Issler, J. V. and Piqueira, N. S. (2000). Estimating relative risk aversion, the discount rate, and the intertemporal elasticity of substitution in consumption for brazil using three types of utility function, *Brazilian Review of Econometrics* **20**(2): 201–239.

Jarrow, R., Li, H. and Zhao, F. (2007). Interest rate caps "smile" too! but can the libor market models capture the smile?, *The Journal of Finance* **62**(1): 345–382.

Kahneman, D. and Tversky, A. (1979). Prospect theory: An analysis of decision under risk, *Econometrica* **47**(2): pp. 263–292.

Kotzé, A. and Joseph, A. (2009). Constructing a South African Index Volatility Surface from Exchange Traded Data.
**URL:** *http://ssrn.com/abstract=2198357 or http://dx.doi.org/10.2139/ssrn.2198357*

Kotzé, A., Labuschagne, C. C., Nair, M. L. and Padayachi, N. (2013). Arbitrage-free implied volatility surfaces for options on single stock futures, *The North American Journal of Economics and Finance* **26**(0): 380 – 399.

Macbeth, J. D. and Merville, L. J. (1979). An Empirical Examination of the Black-Scholes Call Option Pricing Model, *The Journal of Finance* **34**(5): pp. 1173–1186.

Merton, R. C. (1973). Theory of rational option pricing, *The Bell Journal of Economics and Management Science* **4**(1): pp. 141–183.

Merton, R. C. (1976). Option pricing when underlying stock returns are discontinuous, *Journal of Financial Economics* **3**(1–2): 125 – 144.

Mueller, H., Lacoste, G., Zimmerman, D., Ho, T. and Friedman, E. (2002). Managing equity guarantees, *Record of the Society of Actuaries* **28**(1).

Panayiotis, A., Chris, C. and Spiros, M. (2008). Assessing implied volatility functions on the s&p500 index options.
**URL:** *http://papers.ssrn.com/sol3/papers.cfm?abstract/id=1155703*

Peña, I., Rubio, G. and Serna, G. (1999). Why do we smile? on the determinants of the implied volatility function, *Journal of Banking and Finance* **23**(8): 1151 – 1179.

Rubinstein, M. (1985). Nonparametric Tests of Alternative Option Pricing Models Using All Reported Trades and Quotes on the 30 Most Active CBOE Option Classes from August 23, 1976 Through August 31, 1978, *The Journal of Finance* **40**(2): pp. 455–480.

Rubinstein, M. (1994). Implied binomial trees, *The Journal of Finance* **49**(3): 771–818.

Sharpe, W. F. (1964). Capital asset prices: A theory of market equilibrium under conditions of risk*, *The journal of finance* **19**(3): 425–442.

Shreve, S. E. (2004a). *Stochastic Calculus for Finance I: The Binomial Asset Pricing Model*, 1 edn, Springer.

Shreve, S. E. (2004b). *Stochastic Calculus for Finance. II: Continuous-time models.*, New York, NY: Springer.

Taylor, D. (2014). Modelling south african single-stock futures option volatility smiles, *Accepted: Investment Analysts Journal* .

Tompkins, R. G. (2001). Implied volatility surfaces: uncovering regularities for options on financial futures, *The European Journal of Finance* **7**(3): 198–230.

Wakker, P. P. (2008). Explaining the characteristics of the power (CRRA) utility family, *Health Economics* **17**(12): 1329–1344.

# Appendix A

# Relative Risk Aversion of Power Utility

In this section the relative risk aversion (also known as the Arrow-Pratt measure) for the power utility function is derived.

The power utility function, $U$, takes the following form:

$$U(x) = \begin{cases} \dfrac{x^{1-\gamma} - 1}{1-\gamma} & \gamma > 0, \gamma \neq 1 \\ \ln(x) & \gamma = 1 \end{cases}$$

for some level of wealth, $x$.

The relative risk aversion (RRA) of a utility function $U(x)$ is defined as:

$$RRA_U(x) = \frac{-xU''(x)}{U'(x)}$$

The power utility function has the following first and second order derivatives:

$$U'(x) = \begin{cases} x^{-\gamma} & \gamma > 0, \gamma \neq 1 \\ \dfrac{1}{x} & \gamma = 1 \end{cases}$$

$$U''(x) = \begin{cases} -\gamma x^{-\gamma-1} & \gamma > 0, \gamma \neq 1 \\ -\dfrac{1}{x^2} & \gamma = 1 \end{cases}$$

Using these derivatives then gives the following constant RRA:

$$RRA_U(x) = \begin{cases} \frac{x^{-\gamma}\gamma}{x^{-\gamma}} & \gamma > 0, \gamma \neq 1 \\ \frac{\frac{1}{x}}{\frac{1}{x}} & \gamma = 1 \end{cases}$$

$$= \begin{cases} \gamma & \gamma > 0, \gamma \neq 1 \\ 1 & \gamma = 1 \end{cases}$$

# Appendix B

# Theorems of Bakshi *et al.* (2003)

## B.1 Theorem 2 of Bakshi *et al.* (2003)

In this section the derivation of equation (2.17) (Theorem 2 of Bakshi *et al.* (2003)) is shown.

Let $p(R_i)$ be the real-world marginal probability density for the log-return of security $i$, $S^{(i)}$, for $i = 1, ..., N, M$ (where $M$ represents the market index) over the time period $t$ to $T$. In addition, let $p(R_1, ..., R_N, R_M)$ be the joint real-world probability density of all securities and the market index. For ease of exposition, the $R$ will be used to denote $R_M$ In addition, let $q(\cdot)$ similarly represent both the marginal and joint probability densities under the risk-neutral measure. Furthermore, assume a power utility function in wealth.

Let the first four moments of $p(R_M)$ be defined as $\bar{\kappa}_1$,...,$\bar{\kappa}_4$. In other words:

$$\bar{\kappa}_1 \equiv \int_{-\infty}^{\infty} R\, p(R)\, dR$$

$$\bar{\kappa}_2 \equiv \int_{-\infty}^{\infty} R^2\, p(R)\, dR$$

$$\bar{\kappa}_3 \equiv \int_{-\infty}^{\infty} R^3\, p(R)\, dR$$

$$\bar{\kappa}_4 \equiv \int_{-\infty}^{\infty} R^4\, p(R)\, dR$$

Without loss of generality, suppose the physical probability density, $p(R)$ has been mean shifted to have a mean of zero.

Define the moment-generating function, $\bar{\mathscr{M}}(\lambda)$, of $p(R)$, for any real number $\lambda$ by:

$$\begin{aligned}\bar{\mathscr{M}}(\lambda) &= \int_{-\infty}^{\infty} e^{\lambda R} p(R) dR \\ &= 1 + \frac{\lambda^2}{2}\bar{\kappa}_2 + \frac{\lambda^3}{6}\bar{\kappa}_3 + \frac{\lambda^4}{24}\bar{\kappa}_4 + o(\lambda^4)\end{aligned}$$

Similarly, define the moment-generating function of $q(R_M)$ to be, $\mathscr{M}(\lambda)$.

Under certain conditions, by the Radon-Nikodym Theorem, the following identities hold:

$$\begin{aligned}q(R) &= \frac{e^{-\gamma R} p(R)}{\int_{-\infty}^{\infty} e^{-\gamma R} p(R)\, dR} \\ q(R_1, ..., R_N, R) &= \frac{e^{-\gamma R} p(R_1, ..., R_N, R)}{\int_{-\infty}^{\infty} e^{-\gamma R_M} p(R_1, ..., R_N, R)\, dR_1, ...dR_n,\, dR}\end{aligned}$$

where $\gamma$ is the coefficient of relative risk aversion and $e^{-\gamma R}$ is the pricing kernel in power utility economies.

From these identities the following holds:

$$\begin{aligned}\mathscr{M}(\lambda) &= \int_{-\infty}^{\infty} e^{\lambda R} q(R) dR \\ &= \frac{\int_{-\infty}^{\infty} e^{\lambda R_M} e^{-\gamma R_M} p(R)\, dR}{\int_{-\infty}^{\infty} e^{-\gamma R} p(R)\, dR} \\ &= \frac{\int_{-\infty}^{\infty} e^{(\lambda-\gamma) R} p(R)\, dR}{\int_{-\infty}^{\infty} e^{-\gamma R} p(R)\, dR} \\ &= \frac{\bar{\mathscr{M}}(\lambda - \gamma)}{\bar{\mathscr{M}}(-\gamma)}\end{aligned}$$

This links the risk-neutral moment-generating function, $\bar{\mathscr{M}}$, with the real-world (physical) moment-generating function, $\mathscr{M}(\lambda - \gamma)$.

Using the properties of moment-generating functions the following recursive re-

lationship is established, up to a first-order effect of $\gamma$:

$$\begin{aligned}\kappa_1 &\equiv \int_{-\infty}^{\infty} R\, q(R)\, dR \approx \bar{\kappa}_1 - \gamma\bar{\kappa}_2 \\ \kappa_2 &\equiv \int_{-\infty}^{\infty} R^2\, q(R)\, dR \approx \bar{\kappa}_2 - \gamma\bar{\kappa}_3 \\ \kappa_3 &\equiv \int_{-\infty}^{\infty} R^3\, q(R)\, dR \approx \bar{\kappa}_3 - \gamma\bar{\kappa}_4\end{aligned}$$

since $\bar{\mathscr{M}}(-\gamma) = 1 + o(\gamma)$.

Now from the definition of skewness of a distribution, the following results for the risk-neutral skewness of the market, $SKEW_M(t,T)$ :

$$\begin{aligned}SKEW_M(t,T) \equiv & \frac{\int_{-\infty}^{\infty} \left( R - \kappa_1 \right)^3 q(R) dR}{\left\{ \int_{-\infty}^{\infty} \left( R - \kappa_1 \right)^2 q(R) dR \right\}^{\frac{3}{2}}} \\ = & \frac{\bar{\kappa}_3 - \gamma(\bar{\kappa}_4 - 3\bar{\kappa}_2^3)}{\bar{\kappa}_2^{3/2}} + o(\gamma)\end{aligned}$$

By using the fact that $\overline{KURT} \times \bar{\kappa}_2^2 = \bar{\kappa}_4$ and simplifying expression gives the result:

$$SKEW_M(t,T) \approx \overline{SKEW}_M(t,T) - \gamma(t,T)\left(\overline{KURT}_M(t,T) - 3\right)$$

## B.2 Theorem 3 of Bakshi *et al.* (2003)

In this section the derivation for the of equation (2.19) (Theorem 3 of Bakshi *et al.* (2003)) is shown. This involves assuming a single-factor linear return model, however this derivation can easily be extended to that of multi-factor linear models.

Begin by making the assumption that the log-return of security $i$ over the period $t$ to $T$ conforms to the following single-factor model:

$$R_i(t,T) = A_i(t,T) + B_i(t,T)R_F(t,T) + \epsilon_i(t,T) \qquad i = 1, ..., N$$

where $A_i(t,T)$ and $B_i(t,T)$ are constants, $R_F(t,T)$ is the log-return of factor F and $\epsilon_i(t,T)$ is the idiosyncratic component of security $i$'s return. Furthermore, assume

that the expected value of $\epsilon_i(t,T)$ is zero under both the risk-neutral and real-world probability measures and is independent of $R_F(t,T)$

In what follows $\mathbb{E}_t^{\mathbb{Q}}$ will be suppressed to $\mathbb{E}$, $\epsilon(t,T)$ to $\epsilon$ and $R(t,T)$ to $R$ for ease of presentation. Beginning with the definition of security $i$ and using the above assumption the Theorem is derived as follows:

$$\begin{aligned}
SKEW_i(t,T) \equiv & \frac{\mathbb{E}\big[\,\big(\,R_i - \mathbb{E}[R_i]\,\big)^3\,\big]}{\Big\{\mathbb{E}\big[\,\big(\,R - \mathbb{E}\big[R_i\big]\,\big)^2\,\big]\Big\}^{\frac{3}{2}}} \\
= & \frac{\mathbb{E}\Big[\Big(A_i + B_i R_F + \epsilon_i - \big(\,A_i + B_i\mathbb{E}[R_F)]\,\big)\Big)^3\Big]}{\Big\{\mathbb{E}\Big[\Big(A_i + B_i R_F + \epsilon_i - \big(A_i + B_i\mathbb{E}[R_F)]\big)\Big)^2\Big]\Big\}^{3/2}} \\
= & \frac{\mathbb{E}\Big[\Big(B_i\big(R_F - \mathbb{E}[R_F]\big) + \epsilon_i\Big)^3\Big]}{\Big\{\mathbb{E}\big[\big(B_i(R_F - \mathbb{E}[R_F]) + \epsilon_i\big)^2\big]\Big\}^{3/2}} \\
= & \frac{B_i^3\mathbb{E}\big[\big(R_F - \mathbb{E}[R_F]\big)^3\big] + \mathbb{E}[\epsilon_i^3]}{\Big\{B_i^2\mathbb{E}\big[\big(R_F - \mathbb{E}[R_F]\big)^3\big] + \mathbb{E}[\epsilon_i^2]\Big\}^{3/2}}
\end{aligned}$$

since $\mathbb{E}\big[\epsilon_i\big(R_F - \mathbb{E}[R_F]\big)^2\big]$, $\mathbb{E}\big[\epsilon_i^2\big(R_F - \mathbb{E}[R_F]\big)\big]$ and $\mathbb{E}\big[\epsilon_i\big(R_F - \mathbb{E}[R_F]\big)\big]$ are all zero. This then gives:

$$\begin{aligned}
SKEW_i(t,T) = & \Psi_i\, SKEW_F(t,T) + \Upsilon_i(t,T)\frac{\mathbb{E}[\epsilon_i^3]}{\big\{\mathbb{E}[\epsilon_i^2]\big\}} \\
= & \Psi_i\, SKEW_F(t,T) + \Upsilon_i(t,T) SKEW_\epsilon
\end{aligned}$$

where $SKEW_\epsilon(t,T)$ is the skewness of $\epsilon$ and

$$\begin{aligned}
\Psi_i(t,T) &= \left(1 + \frac{e^{r(T-t)}V_\epsilon(t,T)}{B_i^2(t,T)[e^{r(T-t)}V_F(t,T) - \mu_F^2(t,T)]}\right)^{-3/2} \\
\Upsilon_i(t,T) &= \left(1 + \frac{B_i^2(t,T)[e^{r(T-t)}V_F(t,T) - \mu_F^2(t,T)]}{e^{r(T-t)}V_\epsilon(t,T)}\right)^{-3/2}
\end{aligned}$$

# Appendix C

# Results of Chapter 4

## C.1 Results of Section 4.1

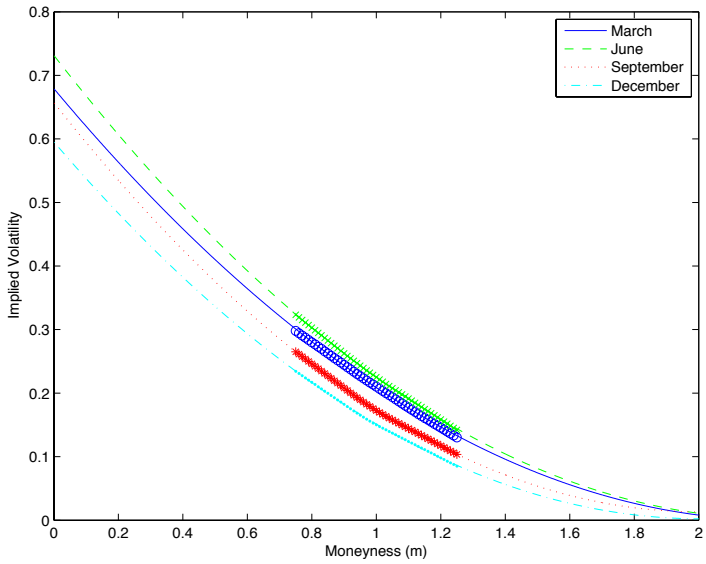


**Fig. C.1:** FTSE/JSE Top40 6-month quadratic volatility smiles for the year 2012 as at March 19, June 18, September 17 and December 18

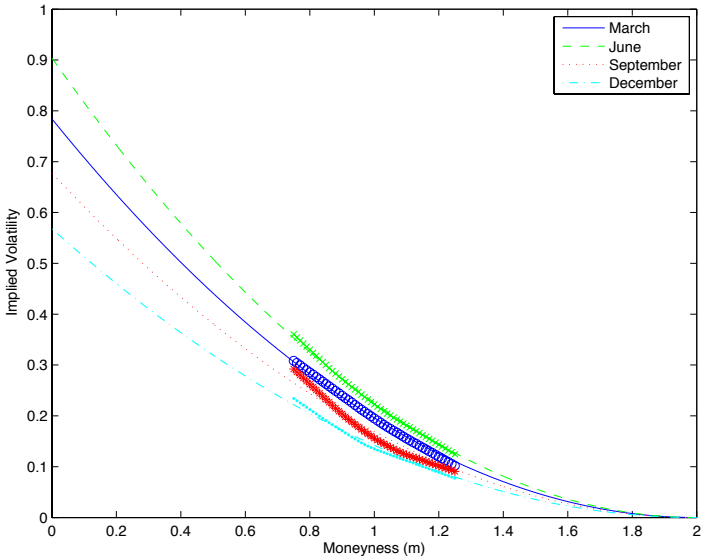


**Fig. C.2:** FTSE/JSE Top40 3-month quadratic volatility smiles for the year 2012 as at March 19, June 18, September 17 and December 18

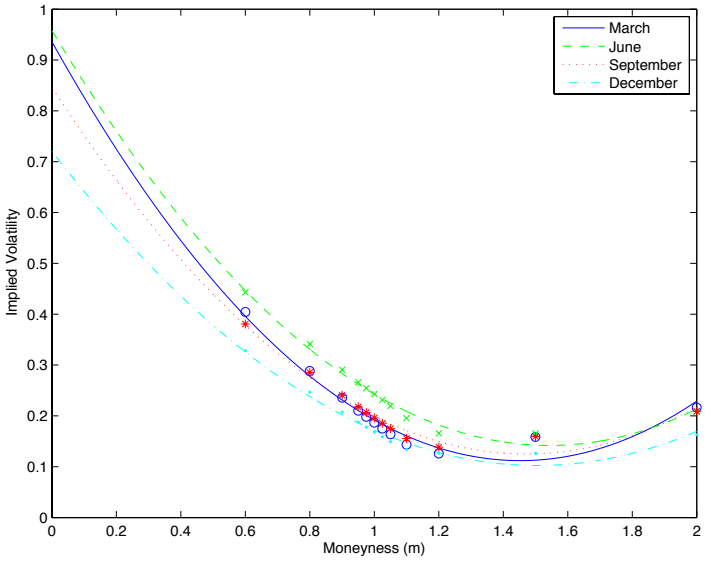


**Fig. C.3:** S&P500 6-month quadratic volatility smiles for the year 2012 as at March 19, June 18, September 17 and December 18

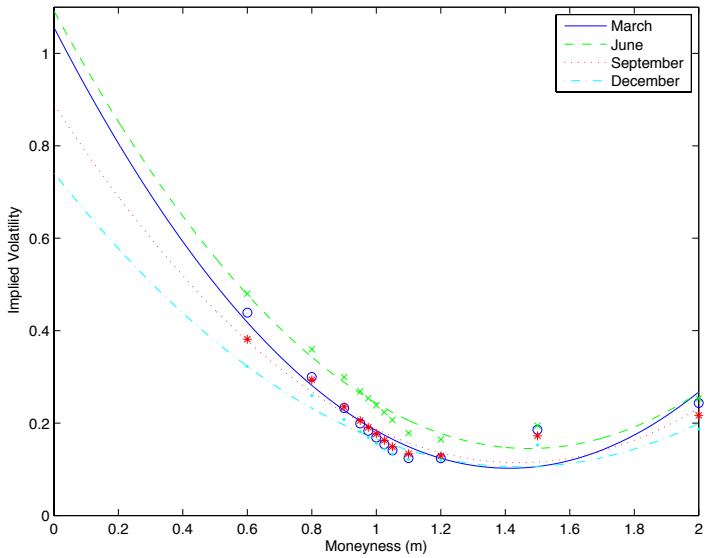


**Fig. C.4:** S&P500 3-month quadratic volatility smiles for the year 2012 as at March 19, June 18, September 17 and December 18

## C.2 Results of Section 4.2

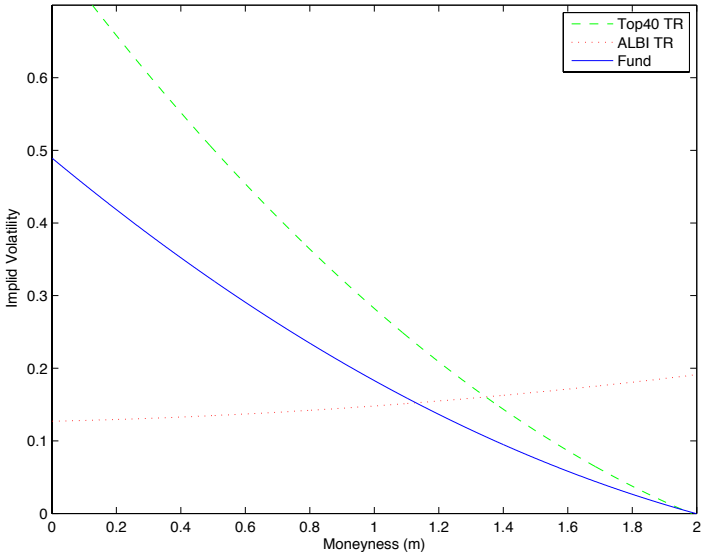


**Fig. C.5:** Volatility smiles of Top40 TR, ALBI TR and the ficticious managed fund as at 18 December 2012 for a maturity of 6 months

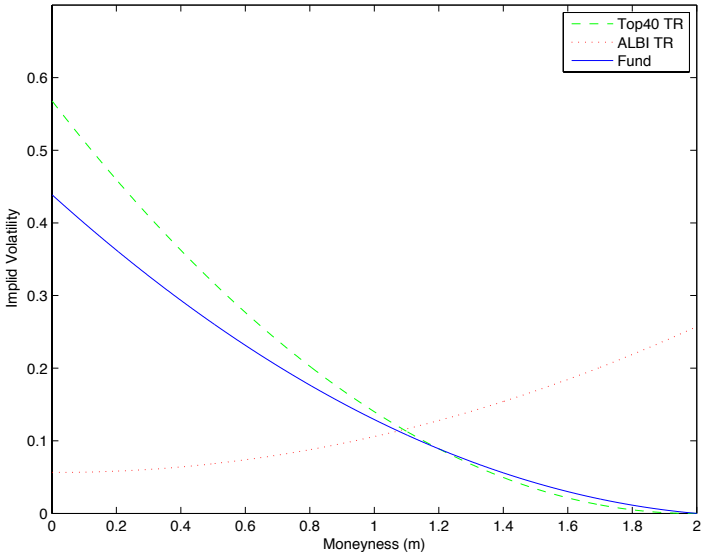


**Fig. C.6:** Volatility smiles of Top40 TR, ALBI TR and the ficticious managed fund as at 18 December 2012 for a maturity of 3 months